



Contents lists available at ScienceDirect

# Engineering Science and Technology, an International Journal

journal homepage: [www.elsevier.com/locate/jestch](http://www.elsevier.com/locate/jestch)

## Effects of shear strength variability on the peak and residual horizontal resistance of on-bottom subsea pipelines in clay

Zeynep H. Özkul<sup>a,\*</sup>, Burak Birgören<sup>b</sup><sup>a</sup> Faculty of Engineering and Natural Sciences, Dept. of Civil Engineering, Yildirim Beyazit University, 15 Temmuz Şehitler Binası, Ayvalı, 151. No: 5 Etlik - Keçiören, Ankara 06010, Turkey<sup>b</sup> Faculty of Engineering and Architecture, Dept. of Industrial Engineering, Kırıkkale University, Ankara Yolu 7. Km, 71450, Yahşihan, Kırıkkale, Turkey

## ARTICLE INFO

## ABSTRACT

**Keywords:**  
 Undrained shear strength  
 Subsea pipelines  
 Peak lateral friction factor  
 Residual lateral friction factor  
 Coefficient of variation  
 R code

Subsea production pipelines in deep water oil and gas fields are susceptible to a phenomenon called lateral buckling which is a major pipeline design concern. Accurate estimation of lateral buckle formation and the additional stresses generated are of particular importance for High-Temperature High-Pressure (HTHP) pipelines resting on soft clay and is the subject of pipe-soil interaction studies (PSI). Variability in pipe embedment and soil resistances constitute the largest uncertainty in PSI analyses. Best practice methods for PSI studies constitute multi-step strategies that involve finding solutions to nonlinear and implicit equations. In the present study, the impact of soil strength variability on embedment and subsequently peak ( $H_{peak}/V$ ) and residual ( $H_{res}/V$ ) lateral friction factors are evaluated. An R code, PSI-Lateral, is developed and verified against published case studies. It is used to calculate the pipeline embedment and horizontal resistances mobilized in a parametric study on three pipe diameters (0.6, 0.8 m and 1.0 m) with three different wall thicknesses. For each pipe diameter-weight combination, embedment and lateral friction factors (peak and residual) are calculated for a series of mean shear strengths ranging from 2 kPa to 8 kPa and COV ranging from 5% to 37.5%. The high estimate and low estimate shear strengths,  $s_{UHE}$  and  $s_{ULE}$ , correspond to values that are +/- two standard deviations from the mean. Hence, the range of strengths encompassed between these two extremes represents approximately 95% of the shear strength distribution. The results of the parametric runs conducted are presented in the form of graphical charts where high and low embedment and lateral friction factors can be read-off for any selected pair of mean shear strength and COV. Similar trends are observed in the charts for all pipelines evaluated. It is found that the range of normalized embedment,  $z/D$ , increases with increasing COV and decreases with increasing mean shear strength for all pipelines tested. A similar trend is observed for the residual horizontal resistance. The expected range of peak horizontal resistance  $H_{peak}/V$  shows the same trend but only for soils with mean strengths less than 4 kPa. For soils with higher mean strengths, the range of  $H_{peak}/V$  is found to be mostly insensitive to variations in COV and further increases in the mean strength.

## 1. Introduction

Subsea pipelines operating under high temperature and pressure (HPHT) tend to expand during operation. Constrained thermal expansion may induce pipeline buckling (or lateral displacement) at specific locations. Such buckles may form as planned or "rogue" buckles along the pipeline route and could lead to overstressing of the pipe wall at the buckle crests. Additional stresses may accrue as a result of displacements associated with startup and shutdown cycles experienced during normal operation. The lateral buckling phenomenon in clays has been rigorously studied over the past decades in order to improve prediction and

design methodologies. Focus has been on identifying key factors and mechanisms which lead to the as-observed embedment in the field and to the formation of lateral buckles (i.e. their spacing and geometry) along given pipeline routes. These have culminated in the development of best practice methods and models for design applications.

Lateral buckling is very sensitive to both the pipe-soil interaction and to features of the as-laid route geometry such as the out-of-straightness and presence of trigger sites (i.e. pipeline segments where soil conditions and/or pipe geometry are particularly favorable to the formation of buckles either naturally or by design). A number of models have been proposed to predict the embedment of pipelines resting on clay seabed.

\* Corresponding author.

E-mail address: [zhokkul.birgoren@aybu.edu.tr](mailto:zhokkul.birgoren@aybu.edu.tr) (Z.H. Özkul).

The PIPESTAB project conducted by SINTEF [27] and projects lead by the American Gas Association/Pipeline Research Committee developed models for use in clays. Models based on empirical evidence were proposed [12,26] and used widely. The HOTPIPE project initiated in 1996 and the SAFEBUCK Joint Industry Project initiated in 2002 have culminated in the development and updates of design and best practice guidelines in the oil and gas industry.

Finite element analysis and plasticity theory have been used to develop models to predict pipeline embedment under combined horizontal and vertical (V-H) loads [13,17,23]. Methods to account for the influence of the soil self-weight and local heave effects were also developed [7,16]. The changes to embedment resulting from large lateral movement of the pipeline were investigated [28].

Centrifuge model tests and advanced image analysis of the recorded deformations have been used to disseminate the complex pipeline deformation patterns experienced during embedment, lateral breakout [7,9], and during large lateral deformation [34]. Parametric finite element analysis has been used to investigate and develop design tools and equations for estimating the limiting bearing forces related to uplift and combined V-H loading of pipelines on clay soil loaded undrained [13] and the change in the horizontal resistance due to the formation of soil berms adjacent to the pipeline during large deformation [34]. The state-of-the-art methodology that has evolved for the determination of pipe-soil interaction is described in general terms in an addendum to API RP 2GEO (2014) and in more detail in the DNV recommended practice for global buckling [10].

The methodologies developed are deterministic in nature. Nonetheless, it is necessary in the design process to account for variability in the numerous input parameters. The inherent variability in the shear strength of soil along a pipeline route can significantly contribute to the overall variability in the design parameters. The inherent variability in the undrained shear strength of a seabed soil can be estimated by sample collection and testing of soils along the planned route and is routinely determined as part of the geotechnical survey. In practice, the high and low estimates of shear strength are selected based on experience but are often arbitrary. In this study the undrained remolded shear strength of a clay,  $s_{ur}$ , is modeled as a normally distributed random variable as follows:

$$S_{ur} \sim N(s_{um} + kz, (cz)^2) \quad (1)$$

where  $s_{um}$  is the remolded shear strength value at mudline,  $k$  is the remolded shear strength gradient ( $k$ ),  $z$  is the depth and  $s_{um} + kz$  is the expected value of  $S_{ur}$ . The standard deviation at depth  $z$  is

$$\sigma_{S_{ur}} = cz \quad (2)$$

In this study the high estimate (HE) and the low estimate (LE) shear strength profiles are located at +/- two standard deviations from the mean. Hence this interval covers about 95% of the strength values observed across the site. The coefficient of variation (COV) by definition is the standard deviation divided by the mean. In the cases considered  $s_{um}$  is equal to zero, and hence the COV is equal to the constant  $c/k$ . These are represented mathematically in equations (3) through (6). This statistical approach is more suited for reliability studies.

$$s_{urBE} = kz \quad (3)$$

$$s_{urHE} = kz + 2cz \quad (4)$$

$$s_{urLE} = kz - 2cz \quad (5)$$

$$COV = \frac{\sigma}{\mu} = \frac{cz}{kz} = \frac{c}{k} \quad (6)$$

In this paper, a review of the literature and best practice methods for PSI analysis is presented. First, the best practice method to estimate embedment is presented followed by methods to predict the peak and

residual lateral soil resistances. This is followed by a parametric study investigating the influence of soil strength heterogeneity, expressed as a coefficient of variation, COV, on the calculated embedment and ultimately the lateral friction factors (peak and residual) of a pipeline resting on a clay seabed. A PSI calculation tool developed for this purpose and written in the R code language has been used in the analysis. Verification of this code is established by comparing calculated embedment and horizontal resistances with those reported from centrifuge model tests and from theoretical methods. The results of the parametric study are evaluated for selected pipeline size and shear strength ranges. The script for the PSI-lateral code is provided in the Appendix. It may be used by those in the industry and researchers who wish to conduct their own sensitivity studies on project specific soil and pipeline properties.

## 2. Background: The role of PSI in pipeline global buckling design

Extensive structural analyses must be performed during the design stage (with the aid of probabilistic, analytic and finite element tools) to assess whether global buckling will lead to excess stress loading at critical points (i.e. at buckle locations, connection spools and sub-sea structures) or to cumulative fatigue damage over the design life. Mitigation measures may then be incorporated into the design at locations where it is deemed necessary.

In deep water field developments seabed soil conditions frequently consist of very soft highly plastic clays. The pipelines are laid directly on the seabed and since they are partially embedded, the pipeline response to operation related thermal loading is significantly impacted by the pipe-soil interaction. Soil resistance acting along the pipeline axis tends to constrain axial expansion and consequently impacts the degree of compressive stress that can be generated. Soil resistance acting perpendicular to the pipeline axis (i.e. lateral direction) tends to stabilize the pipeline against lateral movement. These axial and lateral soil resistances are primarily a function of the pipeline properties (diameter and submerged weight), the degree of embedment, and the amount of shear strength mobilized in the soil. The determination of the resistance of the soil to pipeline movement is called Pipe-Soil Interaction (PSI) analysis.

PSI analysis essentially consists of determining the resistance of the soil to the movement of the pipeline in three mutually perpendicular directions: vertical (i.e. penetration resistance or embedment), axial and lateral directions. A schematic of pipeline embedment and related friction factors is shown in Fig. 1. The pipe-soil resistance in the axial and lateral directions are typically expressed as equivalent non-dimensional friction factors. These are simply the associated resistance force divided by the relevant submerged weight of the pipeline. Depending on the case considered, the submerged weight of pipeline may correspond to the empty, flooded or product filled condition. The friction factors for axial,  $\mu_a$ , and lateral,  $\mu_L$ , directions are not intrinsic soil properties and tend to vary depending on the embedment of the pipeline and the mobilized undrained shear strength,  $s_u$  in the clay seabed.

The PSI parameters  $\mu_a$  and  $\mu_L$  depend on the in-situ soil strength (which may vary if remolded or re-consolidated), the pipe properties (i.e. submerged weight, diameter, roughness and bending stiffness), the lay conditions (i.e. the catenary shape, lay rate, vessel motion and touch down zone dynamics) and the operating conditions (i.e. the rate and timing of startup and shutdown operations). The PSI resistance parameters inevitably have epistemic (global) uncertainty and aleatory (local) variability [36]. The epistemic uncertainty arises from uncertainties associated with (i) determination of the soil strength, (ii) calculation methods/models used for determining PSI parameters and (iii) from operating conditions affecting rate of loading. The aleatory variability arises from (i) geotechnical variability (i.e. varying soil conditions along the pipeline route), (ii) local changes in the lay rate of the pipe and (iii) changing weather conditions and vessel motion during the installation process [30].

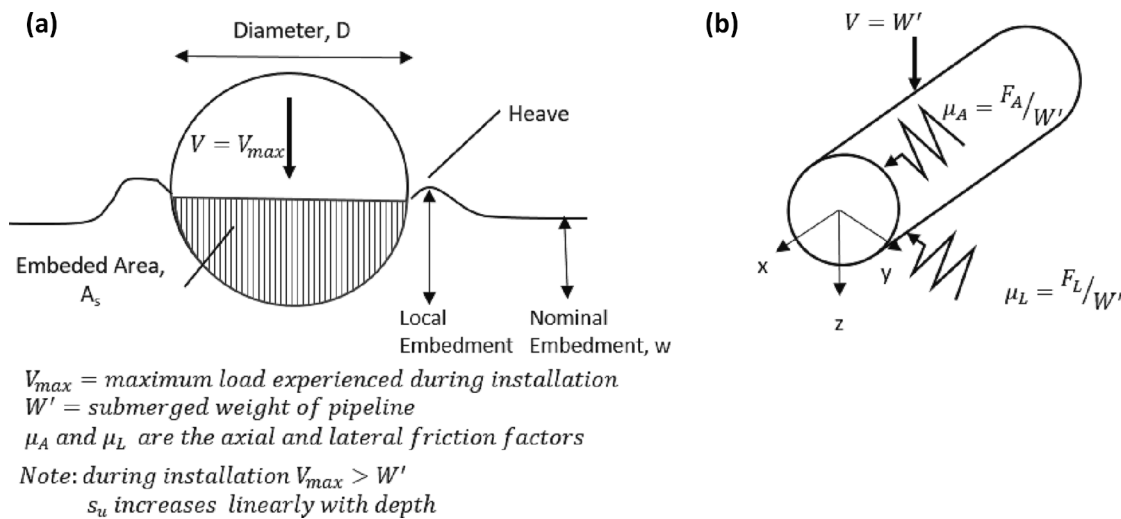


**Fig. 1.** Schematic of on-bottom pipeline on clay seabed (a) profile during installation conditions (b) idealized representation of the soil force acting on a pipeline represented by discrete springs (or friction factors) in two mutually perpendicular directions.

During the design phase the pipeline is checked for various design aspects: end expansions, buckle initiation and response (monotonic and cyclic), walking, route curve pullout and anchoring loads. Depending on the design aspect, either high or low values of PSI resistance can be the most onerous [36]. There is no single “conservative” friction factor that may be used in the analyses which will ensure a “safe” design with respect to all the different design concerns. Low values of soil resistance enable development of large end expansions and high associated stresses. Conversely, high values of resistance tend to promote tighter curvatures at buckle locations which may lead to unacceptable levels of strain [25,31,33].

The potential range of end expansions and strains developed in the buckles need to be determined by considering friction factors based on the full realistic range of pipeline and soil input properties. Low estimate (LE), best estimate (BE), and high estimate (HE) values of each PSI parameter are used in buckling and walking analysis to capture the effect of geotechnical variability and uncertainty along the given route [31]. It has been shown, however, that use of LE, BE and HE values of soil strength in deterministic calculations to identify the range of relevant breakout friction factors can lead to an over- or under-estimation of the actual range. Furthermore, because of the non-linearity of the relationship between soil properties, pipe embedment and lateral resistance, analyses based on arbitrary combinations of LE, BE and HE soil parameters, may not capture the extreme values of the PSI parameters that are actually possible [32,35].

In current pipeline buckling and walking analysis, two different design activities are performed: (1) assessments of buckle initiation which is performed probabilistically and (2) assessments of buckle response which is performed deterministically with the aid of finite element analyses. While rogue buckles can overstress and damage the pipeline, controlled buckle formation can aid the designer in making the pipeline system more economical. It has been stated that a realistic modeling of the interaction between soil and pipeline needs to be integrated into the structural analysis models [8]. Fig. 2 presents a diagram of different processes and calculations involved in pipe-soil interaction studies. Aspects that are part of the geotechnical analysis and those that are part of pipeline design are shown in separate clusters. Realistic modeling of the pipe-soil interaction involves consideration of the different loading stages in the life of the pipeline: installation, pre-commissioning stage (i.e. consolidation and hydrotest) and operation. Refinements in the range of axial and lateral friction factors,  $\mu_A$  and  $\mu_L$ , lead to improved estimations of buckle initiation and pipeline response.

Identifying the range of PSI parameters (LE, BE and HE) that is representative of what will be experienced in the field is an important and challenging design objective. Considerable variability is observed in the as-laid embedment [30,37]. Extensive research efforts have shown that accurate estimation of embedment requires the consideration of multiple factors and that the relationships established between shear strength, embedment and the resulting lateral resistance are non-linear in nature. Hence, quantifying how much variability in lateral resistance

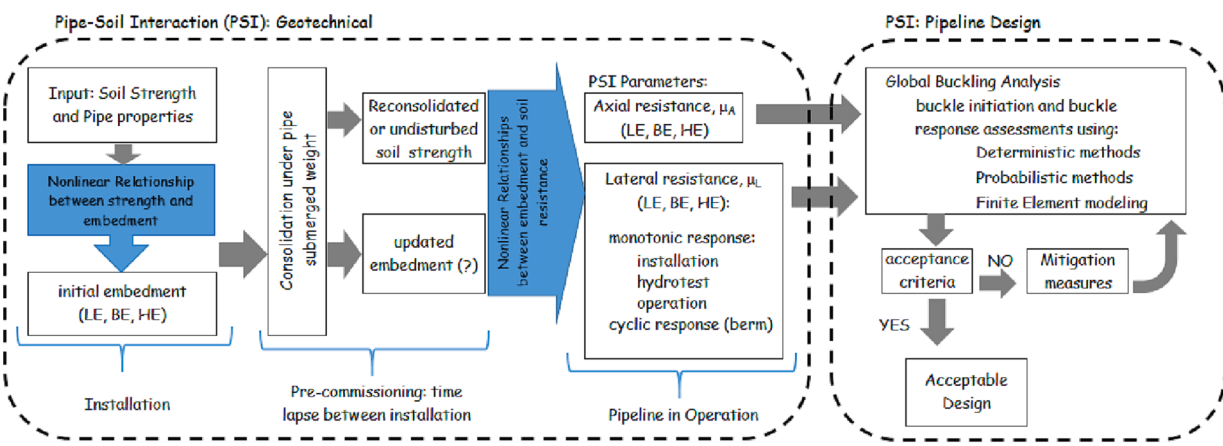


**Fig. 2.** Schematic diagram of PSI analysis which provides necessary input for the global lateral buckling design of offshore pipelines.

will result from a given variability in undrained shear strength is not easily determined.

In the previous section, a brief historical overview of research in pipe-soil interaction was presented. In this section, pipe-soil interaction analysis of on-bottom pipelines resting on clay seabed were discussed taking into consideration factors impacting pipeline embedment. The PSI parameters, or friction factors, which are used in pipeline design checks were introduced. These PSI parameters have significant uncertainty (arising from multiple factors) which must be taken into consideration in the pipeline design process. Soil strength heterogeneity is identified as a significant contributor to this uncertainty and yet the magnitude of its impact is difficult to ascertain because of the complexity of the mathematical models used. For the sake of clarity, a simplified overview of the analysis process to determine PSI parameters (i.e. the axial and lateral friction factors) and the role that these parameters have in the overall pipeline design checks are presented in the form of a flow diagram in Fig. 2.

### 3. Mathematical models and best practice guidelines

The mathematical models that describe the penetration of the pipeline as functions of the properties of the pipe, the seabed soil and the pipe lay conditions are presented in section 3.1. The mathematical models used to predict the resistance to lateral movement of the pipeline are presented in section 3.2. Also discussed in this chapter are certain aspects of current best practice which are:

1. Incorporation into embedment calculations the influence of dynamic effects that occur during the pipe laying process
2. The use of operative shear strength of the clay at the time of loading which will differ from both the undisturbed and remolded strengths
3. Differentiation between “light” and “heavy” pipeline behavior when calculating resistance to lateral motion

#### 3.1. Vertical penetration

The vertical penetration or embedment of the pipe essentially determines the magnitude of the pipe-soil contact area which, in turn, affects the soil resistance that may be mobilized during axial and lateral movements of the pipeline (see Fig. 1). Hence, the degree of embedment impacts both the on-bottom stability and the internal stresses that develop within the pipe cross-section.

A large part of the spatial variability and uncertainty associated with global buckling design is related to the wide range of embedment that is observed along a given pipeline route. Factors affecting pipeline embedment have been identified as soil variability, seabed features, dynamics of the pipe lay process and the prevailing sea state during the installation phase.

Determination of pipeline embedment in clay is complicated by the fact that the undrained strength of clay is not unique. Upper and lower bound plasticity solutions for the embedment problem in clay were presented in different studies [18,23]. These solutions were further extended using finite element analyses [2,16,17]. The culmination of these works is the representation of embedment as a generalized power law relationship between the ultimate vertical load, the pipe shear strength at the pipe invert, pipe outer diameter and the submerged weight of the clay. This solution is presented in Eq. (7). Here the multiplier “6{Prime} and the exponent “0.25” are values suggested for use by Randolph and White [23]. The relationship is in normalized form where  $D$  is the pipe diameter,  $s_{u,invert}$  is the shear strength at the pipe invert,  $z$  is the embedment at the pipe invert,  $V_{ult}$  is the corresponding ultimate vertical load,  $A'$  is the nominal area of the pipe that is below the seabed and  $\gamma'$  is the submerged unit weight of the soil.

$$\frac{V_{ult}}{s_{u,invert}D} = 6\left(\frac{z}{D}\right)^{0.25} + f_b \frac{A'\gamma'}{s_{u,invert}D} \quad (7)$$

$$\frac{V_{ult}}{s_{u,invert}D} = 3.4\left(\frac{10z}{D}\right)^{0.25} + f_b \frac{A'\gamma'}{s_{u,invert}D} \quad (8)$$

The first term in Eq. (7), the power law term, represents the resistance associated with the cohesion of the soil (i.e.  $N_c$  term from bearing capacity theory). This first term tends to over-predict the soil resistance at very low embedment (i.e. when the normalized embedment is less than about 0.1). In such cases the first term should be revised as shown by the expression in Eq. (8). Given a specific pipe section (with known  $D$  and  $V_{ult}$ ) and a soil profile, Eqs. (1) and (2) may be used to estimate the embedment,  $z/D$ , of the soil. For embedment values less than 10% of the diameter (i.e.  $z/D$  less than 0.1) Eq. (2) should be used. This essentially amounts to selecting the minimum of the two equations [23].

In very soft sediments where the soil has been remolded, the contribution of buoyancy to penetration resistance can be significant. The second term in Eq. (7) and Eq. (8) accounts for the added resistance (or uplift) due to the buoyancy along the section of the pipeline embedded in the soil (area  $A_s$  in Fig. 1). The additional penetration resistance due to buoyancy effect is also impacted by the local embedment. The local embedment is the nominal embedment plus the height of heave resulting from the displacement of soil from beneath the pipe bottom towards the sides as penetration occurs. The buoyancy term is multiplied by a factor  $f_b$ , which accounts for this heave. This buoyancy factor has been found to vary linearly with the non-dimensional term  $kD/s_{u,ave}$  where  $k$  is the shear strength gradient and  $s_{u,ave}$  is the average of the shear strengths at mudline and at a depth of one pipe diameter. Based on a parametric finite element study, it has been shown that the value of  $f_b$  could be estimated from the relationship presented in Eq. (9) [7]. An average value of 1.5 may be used for cases where  $kD/s_{u,mudline}$  is equal to 1.

$$f_b = 0.2(kD/s_{u,avg}) + 1.38 \quad (9)$$

The embedment of the pipeline is also affected by properties of the pipeline including its stiffness, lay tension and the shape of the suspended pipeline string during the pipe lay process. Stress concentrations at the touchdown point tend to cause contact stresses that exceed the submerged self-weight ( $W'$ ) of the pipe. The ratio of the maximum contact force between the pipeline and clay (per unit length of pipe),  $V_{max}$ , and the submerged weight of the pipeline is called the local force concentration factor,  $f_{lay}$  (i.e.  $V_{max}/W'$ ). It can be expressed as a function of the seabed stiffness,  $k^*$ , the stiffness of the pipe expressed as  $EI$  and the horizontal component of the lay tension,  $T_0$  as shown in Eq. (10).

$$\frac{V_{max}}{W'} = 0.6 + 0.4\left(\frac{EIW'k_{lay}}{z_{ini}T_0^2}\right)^{0.25} \quad (10)$$

The lay tension,  $T_0$ , shown in Eq. (10) can be estimated using a simple catenary solution of the pipeline string suspended in the water column. The relationship is based on the pipe hang-off angle,  $\phi$ , the water depth to seabed  $z_w$ , and the submerged weight of the pipeline,  $W'$  [22] as shown in Eq. (11).

$$\frac{T_0}{z_w W'} = \frac{\cos\phi}{1 - \cos\phi} \quad (11)$$

For static lay conditions where the horizontal tension  $T_0$  is greater than  $(3\sqrt{EI/T_0} W')^{2/3}$  the value of  $f_{lay}$  may be approximated by Eq. (10) where  $k_{lay}$  is the touchdown lay factor ( $V_{max}/W'$ ),  $W'$  is the submerged weight of the pipe at installation,  $z_{ini}$  is the initial pipeline embedment after laying and  $T_0$  is the horizontal component of the effective lay tension in the pipe at touch-down point during installation [23].

In determining the static pipeline penetration there must be compatibility between the resulting  $V_{max}$  and the vertical resistance

expected at that penetration for the given strength profile. The embedment depth that satisfies this condition may be found by first establishing  $k_{lay,1} = V_{ult}/W'$  with penetration depth based on Eqs. (7) or (8).  $k_{lay,2}$  is found by inserting  $k_{lay,1}$  in the right-hand side of Eq. (10). The compatible embedment and touchdown factor is found when  $k_{lay,1} = k_{lay,2}$  [11].

Inspection of as-laid pipeline embedment are conducted routinely to verify that the embedment values predicted in the design phase are in fact valid. Improved prediction of pipeline embedment is critical to narrowing the range of pipe-soil responses obtained [4]. A number refinements to embedment calculations have been developed. These include (i) methods to account for the dynamic effects of the installation process and (ii) methods to account for strength changes arising from the consolidation of the soil under the pipeline's self-weight (i.e. use of operative strength). These are discussed in the following sections.

### 3.1.1. Embedment – Accounting for dynamic effects

The initial embedment of pipelines is significantly influenced by the dynamics of the installation process itself. The cyclic movements of the pipeline in the vicinity of the touchdown point may be in the vertical and horizontal directions and are caused by the vessel motion and the hydrodynamic loading of the hanging pipeline. These cyclic motions induce full or partial remolding of the seabed clay in the touchdown region leading to significant strength loss, or softening, and result in increased embedment as compared to the "static" case. Typically, the fully remolded strength of clay is about a third of its undisturbed strength. The net result is that field penetrations are much larger than those estimated assuming a "static" penetration (with shear strength of clay close to its undisturbed value). The "dynamic" as-observed embedment in the field can be estimated by using the fully remolded strength of the soil [30]. This is now the accepted practice and has led to the routine measurement of remolded strengths of near-seabed soils using cyclic penetration testing typically with the use of a T-bar or Ball type penetrometer.

Large deformation finite element methods have been used with shear strengths modified for strain rate and softening to study pipe-soil interaction during vertical embedment [7]. It has been found that if both strain rate and softening effects are taken into account, the computed response is a good match with centrifuge data as reported by [9]. It has also been found that water entrainment can increase the soil sensitivity significantly compared to the fully remolded strength measured without water entrainment [24].

The as-laid embedment of pipelines in deep water have also been shown to have a periodic variation with a wavelength equal to the payout length of pipeline (typically 25 m) [30]. This has been attributed to the start-stop payout sequence typically used in pipe laying which gives rise to different sections of the pipeline being subjected to different durations of dynamic lay effects. The variation in embedment was bracketed by calculations that adopted the intact and remolded strength profiles, coupled with the corresponding dynamic force concentration factors.

Field observation studies show that there is considerable variation in the embedment along a pipeline route. Detailed back analysis of as-laid pipeline embedment in soft clayey soil (strength gradients ranging from 0.425 to 0.947 kPa/m) have been conducted along a 45 km long pipeline route in the Bengal Bay [37]. The four sections of the route evaluated were reported to have consisted entirely of either "very soft to firm clay" or "soft clay". Statistical analysis of observed embedment reportedly showed that 80% of the measurements of non-dimensional embedment ( $z/D$ ) were between upper and lower limit ranges of 0.475 and 0.830 depending on route section properties. The values reported were noted to correspond to good weather lay conditions. It was also found that the remolded soil resistance to the pipeline during the dynamic laying process was 0.48–0.74 of the intact soil resistance [37]. Use of the remolded strength is currently a widely used approach and has been adopted in this study.

The magnitude and duration of cyclic motions, and the associated dynamic effect on pipeline embedment, are closely related to the severity of weather conditions experienced during the pipe laying process as well as to the occurrence of any downtime periods (i.e. pauses in pipe laying due to equipment failure). Increased severity in weather conditions and longer downtime are associated with higher degrees of remolding and softening of the clay and higher recorded embedment. Although it is not possible to know a-priori what the weather conditions will be during pipe lay, a certain degree of dynamic effect can be taken into account in the design process. This may be achieved in one of two ways: 1) the submerged weight of the pipe may be multiplied by an adjustment factor  $f_{dyn}$  (typically taken as a factor of two) before calculating embedment, or 2) a "static" embedment calculation may be performed using the fully remolded shear strength profile and without any other adjustment for dynamic effects.

Comparison of calculated and as-observed field embedment values have shown that the latter approach provides reasonable estimates of field embedment values for pipelay occurring during average weather conditions. This approach has been found to over-predict values of embedment in the case of pipelay occurring in very calm weather conditions and under-predict values of embedment during pipelay in extreme weather conditions and in pipelay conditions associated with down time events [29,30]. In summary, use of the remolded shear strength in place of the undisturbed strength allows for an improved estimation of pipeline penetration as-observed in the field.

### 3.1.2. Embedment – Accounting for operative strength

After installation the soil supporting the pipeline will begin to consolidate under the submerged (usually empty) weight of the pipeline. The shear strength of these near seabed clays is in the order of a few kilopascals and they typically have liquidity indices larger than one. Hence, any change in the consistency due to consolidation can significantly impact the pipe-soil interaction. There is a time lapse between installation of the pipeline and hydrotest phase. This period typically lasts for several months or more, and hence there is sufficient time for the soil to reconsolidate under the as-installed submerged weight of the pipeline. Further embedment of the pipeline may occur during the hydrotest phase if the increase in the submerged weight of pipeline due to flooding is significant. It was proposed [4] that calculation of additional pipeline embedment (associated with the increased load during the hydrotest phase) should be made using the "operative" shear strength of the soil instead of the undisturbed strength. This "operative" reconsolidated strength is based on the normally consolidated shear strength ratio and the vertical stress generated by the pipe before flooding. The normally consolidated shear strength ratio of the clay can be determined by laboratory testing.

## 3.2. Peak and residual lateral resistances in undrained loading

Once an HPHT pipeline is operational, the hot and pressurized contents will induce pipeline expansion leading to the formation of buckles at intervals along the route. A shut-down in production will cause contraction and the pipeline will tend to move back towards its original as-laid position. Subsequent start-up and shut-down cycles in operation cause the pipeline to cycle back and forth along the seabed at the buckled locations possibly leading to the formation of soil berms. This large displacement response of the pipe-soil system to operational load cycles is generally evaluated in two phases: (i) a monotonic response phase and (ii) a cyclic response phase. These are depicted in Fig. 3 as the blue and green curves respectively. In the monotonic response, a breakout resistance occurs at peak shearing resistance of the soil followed by large lateral displacement with reduced resistance until a final steady or residual resistance is reached.

In the second phase (i.e. cyclic response phase) the pipe-soil response is characterized by the growth of soil berms at the limits of the pipe displacement range with the pipe descending into a shallow trench. This

study concerns only the first phase, the monotonic response to the first load which consists of the breakout and residual lateral resistances.

The equations used for peak (or breakout) lateral resistance,  $F_{LBOU}$ , and the residual lateral resistances are shown in Eqs. (12) and (13) [33], DNV-RP-F114:

$$F_{LBOU} = \left[ 1.7\left(\frac{z}{D}\right)^{0.61} + 0.23\left(\frac{V}{Ds_{uin}}\right)^{0.83} + 0.6\left(\frac{\gamma' D}{s_{uin}}\right)\left(\frac{z}{D}\right)^2 \right] Ds_{uin} \quad (12)$$

$$F_{L,res,u} = \left[ 0.32 + 0.8\left(\frac{z}{D}\right)^{0.8} \right] V \quad (13)$$

In these equations  $V$  is the static vertical pipe-soil submerged weight for the condition considered (i.e. operation),  $z$  is the pipe embedment,  $D$  is the pipe outer diameter,  $s_{uin}$  is the soil undrained shear strength at the pipe invert depth and  $\gamma'$  is the soil submerged unit weight at the pipe invert depth. In Eq. (12), the first term reflects the passive resistance related to the soil berm pushed in front of the pipeline. The second term is a frictional component and the third term captures the passive self-weight resistance from the soil ahead of the pipe. Alternative models for calculating the lateral residual resistance are provided by [3] and [6].

The relationships in Eqs. (12) and (13) are based on best fit models developed from the results of 67 tests conducted on pipes resting on very soft West African clays [11]. The associated shear strengths range from 0.4 kPa to 9 kPa at mudline and the pipelines are noted to have nominal bearing pressures,  $V/D$ , between 1 kPa and 7 kPa (DNV-RP-F114). It is noted that the undrained shear strength of the soil is not a parameter included in the mathematical expression for the residual lateral undrained horizontal resistance shown in Eq (13). Rather, the effect of undrained shear strength is seen indirectly through the normalized embedment ( $z/D$ ).

Two characteristic types of large-amplitude lateral response have typically been observed in the large-scale tests conducted. At locations where the pipeline buckles, the pipeline translates laterally across the seabed and, as it does, it tends to "correct" for any over- or under-

penetration that may have occurred during installation by either rising up or embedding further into the soil. "Light" pipelines tend to rise after breaking out from their as-laid positions whereas "heavy" pipelines tend to move downward in the soil after breakout (leading to a continuous increase in lateral resistance) and a residual resistance value is not reached [5]. "Light" pipe response is caused in part by the over-penetration that occurs as a result of dynamic effects. The ratio of the pipeline weight to the seabed strength, expressed as  $W/Ds_u$ , is an approximate indicator of which type of response may be expected. In clayey soils, 'light' pipe behavior is generally observed for  $W/Ds_u$  values less than about 2 [1,33]. This corresponds to cases where the pipe-soil vertical force is less than approximately half of the ultimate vertical bearing capacity as calculated at a penetration of half a diameter [11]. This is not a strict limit but indicates the need for additional caution when this limit is approached. The monotonic behavior of a "light" pipe is as shown in Fig. 3.

It is noted that the data set used in developing Eq. (12) for peak lateral resistance includes 5 tests which displayed heavy pipe behavior. Conversely, the empirical expression used for determining residual resistance, Eq. (13), is based on calibrations from a test data set composed mostly of 'light' pipelines. Hence, this expression is not applicable for predicting 'heavy' pipe behavior.

In this section, the mathematical models and current best practice procedures used in PSI analysis have been presented. First, determination of vertical penetration and methods to account for dynamic effects have been discussed (section 3.1). Then, the lateral displacement behavior of HPHT pipeline segments where global buckling occurs is discussed. Differentiation is made between the monotonic and cyclic deformation patterns that are expected as a result of repeated startup-shut down cycles experienced during operation. The empirical equations for the determination of peak and residual lateral resistances expected during the monotonic response of the pipeline to operational loading has been presented (section 3.2).

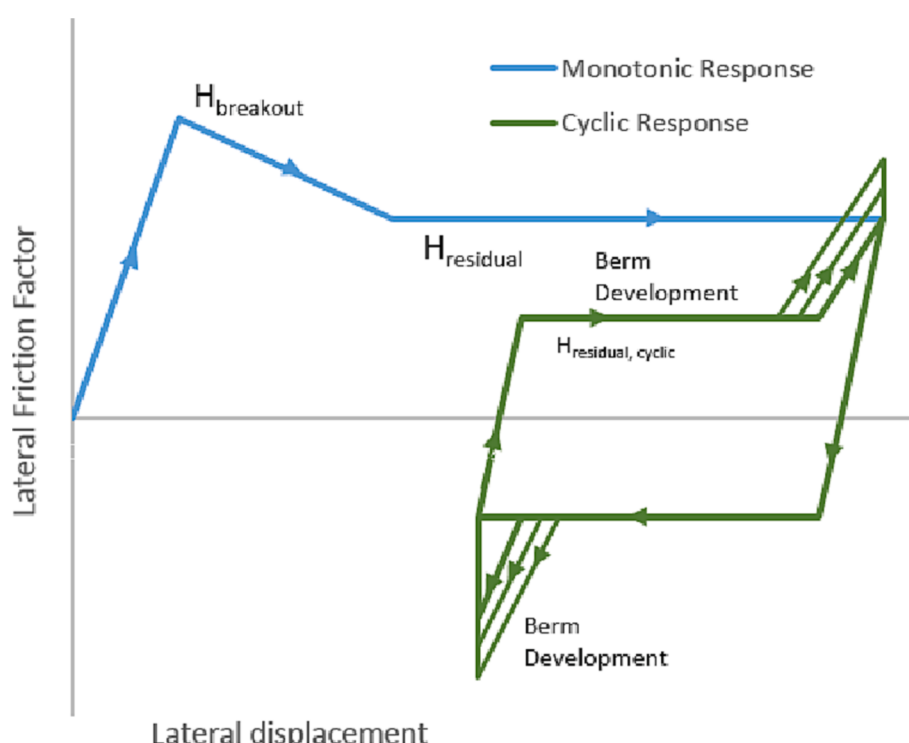


Fig. 3. Idealised pipe-soil response showing load vs lateral displacement of a pipeline: monotonic response (in blue) and cyclic response (in green).

#### 4. Methodology – Parametric study using PSI code

The mathematical models used for initial embedment are implicit in form and must be solved through iteration. Additionally, the associated relationships (i.e. between  $s_u$  and embedment and embedment and PSI factors) are nonlinear making it difficult to foresee the impact of  $s_u$  variability on PSI parameters  $\mu_{peak}$  and  $\mu_{res}$  (see Fig. 1). Yet pipeline design aspects such as buckle initiation are very sensitive to the range of values that these two parameters take. The objective of this study is to investigate the influence of variability in undrained remolded shear strength ( $s_{ur}$ ) on the peak and residual lateral friction factors for pipelines laid on soft clay seabed.

In order to achieve this, an R code was developed to perform the PSI calculations based on the mathematical model and best practice guidelines as described in section 3. The results obtained from the developed code, PSI-Lateral, have been verified using published data from the literature. This verification is for calculated embedment values as well as for calculated peak and residual resistances. The verified code, PSI-Lateral, was then used to conduct a parametric study to evaluate the impact of strength variability on the lateral response of pipelines of different diameters and weights. Details for all of these steps are described in the following sections.

##### 4.1. The developed PSI-lateral code

The R coding language has been selected as the source code for PSI-Lateral. It is one of the most popular open source programming languages for statistical computing. It is an interpreted language, so the R code can easily be run in different platforms without any need for compilation.

The PSI-Lateral code developed calculates the pipeline embedment, peak lateral resistance and residual lateral resistances as described in the previous sections. It consists of essentially four sections: a section where function definitions are made, a section for entering input values, a section with nested for loops for conducting the series of runs identified in the inputs and a section for writing the results to a file. A listing of the R code for “PSI-Lateral” is provided in the Appendix. Verification/validation of the developed PSI code is presented through comparisons with results published in the literature. These include centrifuge test results, reported analytical bearing capacity solutions and observed field embedment values. These are discussed in the following sections.

The calculation of embedment involves finding the equation with the minimum  $V_{ult}/W$  value from Eqs. (7) and (8), and then equating  $V_{ult}/W$  in this equation to  $V_{max}/W$  in Eq. (10). Solving the resulting equation for normalized embedment ( $z/D$ ) requires using an iterative root-finding procedure. This iterative procedure, however, is conducted internally within the coded functions.

##### 4.2. Verification of calculated embedment from PSI-lateral code

The single most important variable impacting the degree of horizontal resistance (peak or residual) that may be developed, is the pipeline embedment. Since horizontal resistance is sensitive to embedment it is important to ensure that estimates of embedment are as accurate as possible and conform to accepted best practice. For this reason, the PSI-Lateral script for embedment is validated against two types of data published in the literature. These include lab data obtained from centrifuge tests and as-laid pipeline embedment obtained from field surveys. Since the calculation methods are nonlinear and involve solutions based on iterative procedures, it is good practice to ensure that the code runs correctly and produces expected results. Verification has been used by the authors as a reality check for the developed code and is provided here for the benefit of interested users.

The centrifuge test reported by Dingle et al. [9] depicts the penetration of a pipe of diameter 0.8 m into a clay with a mudline strength intercept ( $s_{um}$ ) of 2.3 kPa and a strength increase gradient of 0.36 kPa/

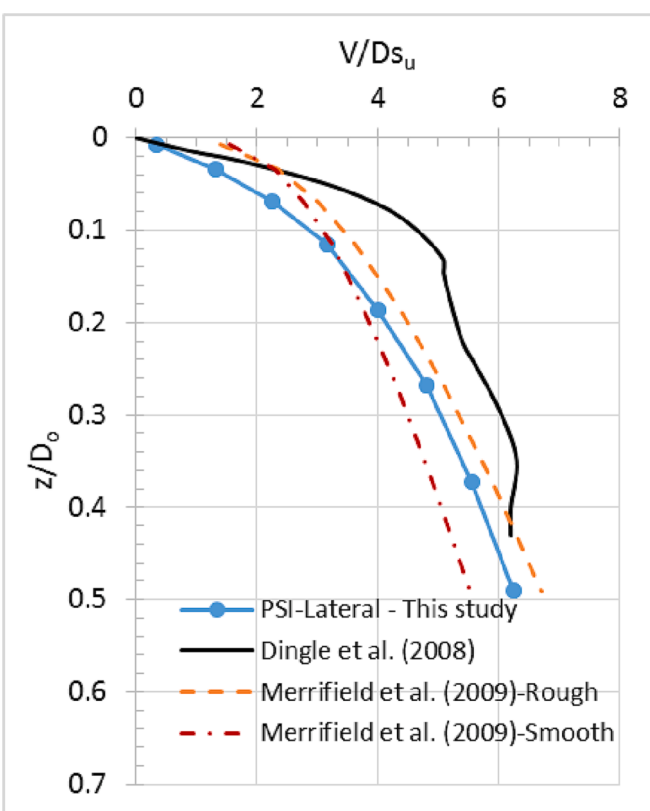


Fig. 4. Normalized penetration resistance versus normalized embedment comparison of values from the literature and those calculated by PSI-Lateral code.

m. The results of this test (shown by the black line) are presented as the normalized vertical force ( $V/Ds_u$ ) versus the normalized embedment ( $z/D_o$ ) in Fig. 4. The calculations from runs conducted for the same pipe-soil combination with a series of increasing vertical loads (i.e. submerged weight) is presented as the blue line in Fig. 4. Comparison of these two lines indicate that the PSI-Lateral code results are reasonably close to those obtained by experiment and generally follow the same trend. It is further noted that the PSI-Lateral code predicts embedment that is slightly higher than that observed in the centrifuge test at identical normalized vertical loads. Conversely, the centrifuge test results give the highest penetration resistance at all normalized embedment larger than about 0.4. This result is reasonable and expected since the method recommended by DNV is calibrated against observed field test results which include dynamic effects that are not present in the centrifuge tests.

The results of PSI-Lateral embedment estimates were also compared to those obtained from back calculated bearing capacity factors as proposed by [16]. These bearing capacity factors had been derived from the results of a series of large deformation finite element analyses. The bearing capacity factors have been reported for rough and smooth pipes. The reader should refer to the original paper for the formulations. The results of these calculations are shown by the yellow and orange dotted lines in Fig. 4. It is observed that for normalized embedment values between 0.2 and 0.5 (which are typical of deep water on-bottom pipelines) the results of the PSI-Lateral code fall in-between the normalized vertical resistances calculated for smooth and rough pipes. This is as expected and further ensures the validity of the code. It should be noted that the bearing capacity factors derived by [16] are valid up to a normalized embedment of 0.5.

The calculations from PSI-Lateral were also compared with field observations of embedment as reported by Zhao et al. [37]. They report field embedment values for a deep water pipeline consisting of two

**Table 1**

Input Values from Zhao et al. [37].

Pipe Section -	$\gamma'$	$S_{um}$	$k$	$S_u/S_{ur}$	$D$	$V$	$I_s$
Estimate Type	$\text{kN/m}^3$	$\text{kN/m}^2$	$\text{kN/m}^2/\text{m}$				
1 - BE	6.37	0	0.947	3	0.883	2.823	0.008805
2 - BE	5.42	0	0.725	3	0.908	4.029	0.01047
3 - BE	5.43	0	0.425	3	0.908	4.029	0.01047
4 - BE	6.09	0	0.525	3	0.908	4.029	0.01047

$E_s = 2 \times 10^8 \text{ kN}$ ; Lay tension = 1800 kN; BE = Best Estimate;  $S_{um}$  = shear strength at mudline;  $k$  = shear strength gradient;  $S_u$  = undrained shear strength;  $S_{ur}$  = remolded shear strength;  $D$  = pipeline outer diameter;  $V$  = submerged pipeline weight at installation;  $I_s$  = second moment of inertia of steel section.

cross-sections and four separate zones of soft clay characterized by different shear strengths. The related soil and pipe characteristics are reproduced in Table 1. Field observations of embedment (minimum, maximum and average value) were reported for the four soil zones. These are shown as the grey, blue and yellow bars in Fig. 5. The embedment predicted using the PSI-Lateral is shown as the orange crosses (connected by orange lines) in Fig. 5. The remolded shear strength ( $S_{ur}$ ) was derived from the undisturbed strength profile ( $S_u$ ) and an assumed sensitivity ( $S_u/S_{ur}$ ).

The embedment results from PSI-Lateral fall within the range bounded by the minimum and maximum observed embedment in the field for all four pipe sections. For pipe sections 2 and 4 the calculated values lie very close to the reported average value. This good match is an indication that the calculated embedment is a good predictor of the as-laid field embedment.

Also shown in Fig. 5 (as green dots connected by solid green lines) is the theoretical normalized embedment as reported by [37] for the four pipe sections. These theoretical embedment values have been noted to be based on the undisturbed shear strength and hence do not account for any dynamic effects. As expected, these embedment values are significantly lower than the field observed average value and lie close to or even lower than the field observed minimum normalized embedment. Comparison of the two line plots further reinforce the importance of taking into account the impact of cyclic loading during installation (which is achieved by using remolded shear strengths) when predicting pipeline embedment. The verification of embedment against published lab and field data establish that the PSI-Lateral code provides acceptable estimates of embedment based on current best practice.

#### 4.3. Verification of peak and residual horizontal resistances from PSI lateral code

The verification of calculations for the peak horizontal resistance obtained using the PSI-Lateral code is shown in Fig. 6. The experimental results reported from the centrifuge test [9], shown as a black line, is for

an initial pipe embedment of about 0.43 pipe diameters. Note that the horizontal resistance to movement,  $H$  (measured as a force per unit length of pipe), is normalized using the undrained shear strength of the soil at the pipe invert times the pipe diameter. As the pipe is pushed laterally, a peak resistance is observed (associated with the development of suction pressures behind the pipe) followed by a sharp decrease in resistance and a gradual rising of the pipe to a normalized embedment of about 0.25 pipe diameters. The horizontal bearing capacity solutions derived by Merrifield et al. (2008) for smooth and rough pipes are also shown and appear to be in good agreement with the peak normalized resistance observed at low horizontal displacement of the pipe.

The results for peak lateral resistance determined using the PSI-Lateral code are also shown in Fig. 6 as the blue solid line with dot markers. The peak normalized resistance increases as a function of normalized embedment depth. The residual resistance is shown by a triangular marker and is calculated at the final normalized embedment of about 0.04 which corresponds to that observed at the end of the centrifuge test. The peak horizontal resistance ( $H/Ds_u$ ) estimate for the initial normalized embedment of 0.43, is in good agreement with the peak measured resistance reported by [9]. The calculated normalized residual resistance is less than that observed by experiment in the centrifuge device but is, as expected, significantly lower than the peak value.

Also shown in Fig. 6 are the error ranges for lateral resistance as based on a model uncertainty factor for Eq. (12) equal to 1.5. The model uncertainty is the uncertainty associated with the scatter around the fit between measured and calculated resistance when empirical methods are applied.

#### 4.4. Parametric analysis

The PSI-Lateral code was used to calculate the peak and residual resistances for a number of combinations of pipeline diameter, submerged pipe weight and mean soil strength as shown in Table 2. Three pipe outer diameters (0.6 m, 0.8 m and 1.0 m) were selected for analysis.

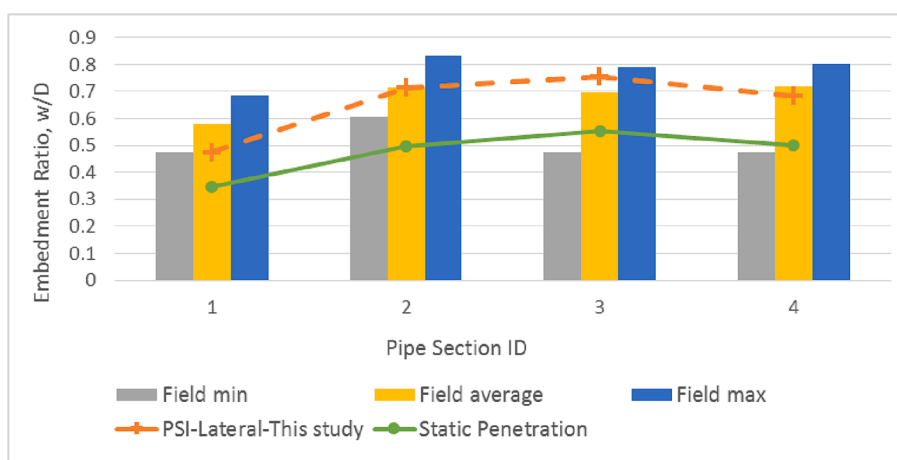
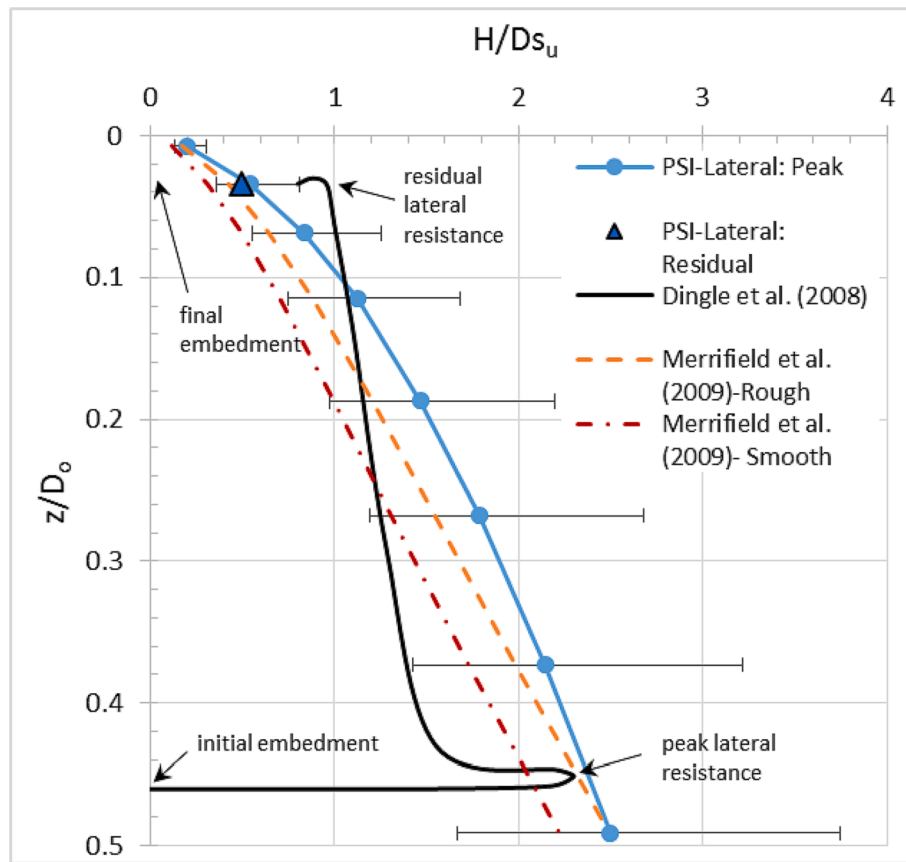


Fig. 5. Comparison of calculated embedment with field survey data from [37].



**Fig. 6.** Verification of normalized peak and residual horizontal resistance estimates using model test results [9] and bearing capacity envelopes [16].

**Table 2**  
Parametric Study.

$k$ (mean $s_{ur}$ gradient) (kPa/m)	$\gamma'$ (SUW) (kN/m <sup>3</sup> )	$S_t$	Coefficient of Variation (COV)	$D$ (m)	$t_s$ (mm)	$W_i/D$ (kN/m <sup>2</sup> )
2, 3, 4, 5, 6, 7, 8	4	3	0.05, 0.075, 0.10, 0.125, 0.15, 0.175, 0.20, 0.225, 0.25, 0.275, 0.30, 0.325, 0.35, 0.375	0.6	25, 27, 30	1.17, 1.62, 2.29
2, 3, 4, 5, 6, 7, 8	4	3	0.05, 0.075, 0.10, 0.125, 0.15, 0.175, 0.20, 0.225, 0.25, 0.275, 0.30, 0.325, 0.35, 0.375	0.8	30, 35, 40	0.80, 1.93, 3.05
2, 3, 4, 5, 6, 7, 8	4	3	0.05, 0.075, 0.10, 0.125, 0.15, 0.175, 0.20, 0.225, 0.25, 0.275, 0.30, 0.325, 0.35, 0.375	1.00	40, 45, 50	1.57, 2.70, 3.81

Note:  $\gamma'$  = submerged unit weight;  $S_t$  = soil sensitivity;  $D$  = pipe outer diameter;  $t_s$  = pipe wall thickness;  $W_i/D$  = pipe nominal stress

For each pipe diameter three wall thickness were selected so as to give three different pipe nominal stress levels.

In the calculation of the initial embedment, the dynamic effects of the lay process are taken into account by using the remolded shear strength of the soil. The remolded undrained shear strength is represented by a shear strength gradient,  $k$ , and a standard deviation,  $\sigma_{Sur} = cz$  (see Eq. (2)). In all the cases considered the remolded strength profile consisted of zero strength at mudline (i.e.  $s_{um} = 0$ ). In order to determine the effect of soil variability many combinations of remolded shear strength and coefficient of variation, COV, were included in the analyses. The mean  $k$  and COV combinations that were run are shown in Table 1. Also shown in Table 1 is the pipe nominal stress which is the submerged empty weight of the pipeline divided by its outer diameter,  $W_i/D$ . It represents the pipe load on the soil when embedded to half its diameter.

The low estimate,  $s_{uLE}$ , and high estimate,  $s_{uHE}$ , strengths for a given combination of  $k$  and COV values are calculated based on Eqs. (3) to (6). In the PSI-lateral code, the value of  $c$  is calculated based on the selected

values of  $k$  and COV. Hence, in this study where the maximum COV is 37.5%, the minimum  $k$  is 2 kPa/m and the maximum  $k$  is 8 kPa/m, the extreme values of  $s_{uLE}$  and  $s_{uHE}$  that have been evaluated are 0.5 kPa/m and 14 kPa/m respectively.

The PSI-Lateral code uses variable names for all soil and pipe parameters that are needed in the calculations. In the parametric study conducted, constant values (default values) were used for a number of these variables. The shear strength at mudline is taken as 0 kPa. The submerged unit weight of the soil is 4 kN/m<sup>3</sup> and the ratio of undrained shear strength to remolded shear strength (or sensitivity) is 3. The Young's modulus of steel is 200 GPa. An arbitrary water depth (i.e.  $zw$ ) of 2000 m is used since soft clay seabed conditions are likely to be found at such water depths. It is noted, however, that the developed PSI code allows for other values to be entered for general applicability.

Calculated parameters in PSI-Lateral include the submerged weight of the pipeline at installation (i.e. empty weight),  $W_i$ , and the section modulus,  $I$ , based on the chosen pipe outer diameter and wall thickness. The lay tension is calculated for typical values of the hang-off angle and

water depth which are arbitrarily chosen for this study as 70 degrees and 2000 m respectively.

There is a significant time lag between the installation of a pipeline and its operation. During this period there is time for (i) any excess pore pressures developed during installation to dissipate, (ii) the soil to consolidate under the additional load of the submerged weight of the pipe and (iii) soil setup to occur. As a result, the shear strength of the soil at the time the pipeline is operational is expected to be higher than that mobilized during the installation stage. This operational strength may be higher or lower than the original in-situ undisturbed shear strength of the soil and is dependent on the submerged weight of the pipeline and consolidation characteristics of the soil.

In the PSI-Lateral code, the undisturbed shear strength at the depth of the pipe invert is used in calculating the lateral resistances. For the purposes of this study, the shear strength relevant at the time of operation is taken to be a multiple of its remolded shear strength at installation. This multiplier,  $s_u_{sur\_ratio}$ , is used to express the general strength gain that occurs in this time period. It can be likened to the soil sensitivity (ratio of undisturbed strength to remolded strength), but is not necessarily limited to the original undisturbed shear strength (since the final shear strength may be higher due to consolidation effects).

In the analyses conducted, the effect of the consolidation and time lapse are assumed to be such that the soil returns to its original undisturbed strength. This is calculated in the code as the product of the remolded strength times the  $s_u_{sur\_ratio}$  which is taken to be equal to 3.

In the parametric study conducted, the ratio of the pipeline weight to the seabed strength,  $V/Ds_u$ , changes as the soil strength is varied. The value of  $V/Ds_u$  has been checked to see whether ‘light’ pipe behavior is expected for the pipe-soil combinations used in this study.

In this section, the methodology used in this study has been presented. First, the PSI-Lateral code that has been developed for this study has been discussed (section 4.1). Then the calculated embedment values from PSI-Lateral have been verified against published case studies in the literature (section 4.2). The calculated monotonic lateral resistances (both peak and residual) have been verified against centrifuge model test results (section 4.3). Finally, the details of the parametric study that has been conducted using PSI-Lateral has been presented (section 4.4).

## 5. Results

In order to be able to compare different cases, the results of the calculations are presented in non-dimensional units. Hence the embedment of the pipeline is presented as the normalized embedment ( $z/D$ ), and the horizontal resistances are presented as pipeline friction factors. The friction factor is a design parameter used in the evaluation of the stability of on-bottom pipelines. It is the expected resistance of the soil to the movement of the pipeline expressed as a ratio of the submerged weight of the pipeline itself. The friction factors for lateral displacement which include the peak (or breakout) resistance ( $H_{peak}/V$ ) and the residual resistance ( $H_{res}/V$ ), are evaluated in this study.

Fig. 7 through Fig. 9 show the calculated normalized embedment ( $z/D$ ) for different mean strength gradients (i.e.  $k$  values) and their family of related high and low shear strength variants ( $s_{uLE}$  and  $s_{uHE}$ ) corresponding to different COV values. In these plots the normalized embedment shown at a COV equal to zero represents the embedment for the mean strength gradient  $k$  and corresponds to the best estimate value of shear strength ( $s_{uBE}$ ). Each series, consisting of embedment values corresponding to a mean  $k$  and its  $s_{uLE}$  and  $s_{uHE}$  variants, is represented by a different color.

In Fig. 7 through Fig. 9, the difference between the normalized embedment corresponding to  $s_{uLE}$  and  $s_{uHE}$  in a given series represents the range of embedment corresponding to shear strengths that lie within +/- two standard deviations of the mean strength  $k$ . The range of embedment, or the prediction interval length ( $PIL$ ) grows as the COV increases. The HE and LE arms of each series produce a kind of side-turned V-shape. It can be seen that as the mean  $k$  value increases, the

apex of the ‘side-turned V’ series moves to lower  $z/D$  values causing the whole series to generally translate upward.

For a given pipeline weight (i.e.  $V = W'$ ), diameter ( $D$ ), and soil unit weight ( $\gamma'$ ), Eq. (12) for calculating  $H_{peak}$  reduces to a relationship that is a function of the normalized embedment and the shear strength at the pipe invert,  $s_{u,invert}$ . Since  $s_{u,invert}$  is determined by the strength gradient  $k$  and the normalized embedment,  $H_{peak}$  is also determined by the strength gradient and normalized embedment. This unique relationship is expressed graphically by the red curves in lateral resistance factor plots of Figs. 5, 6 and 7. The discontinuity observed at a normalized embedment of about 0.1 in the red curve arises from the use of Eq. (8) instead of Eq. (7) for embedment values less than 0.1. The COV vs  $z/D$  chart (on the left) and the lateral resistance factor vs  $z/D$  chart (on the right) may be used together to estimate the  $H_{peak}/V$  value corresponding to a given combination of mean strength gradient  $k$  and COV. First read off the  $z/D$  value from the COV vs  $z/D$  chart and then read off the corresponding  $H_{peak}/V$  value(s) from the  $H/V$  vs  $z/D$  chart.

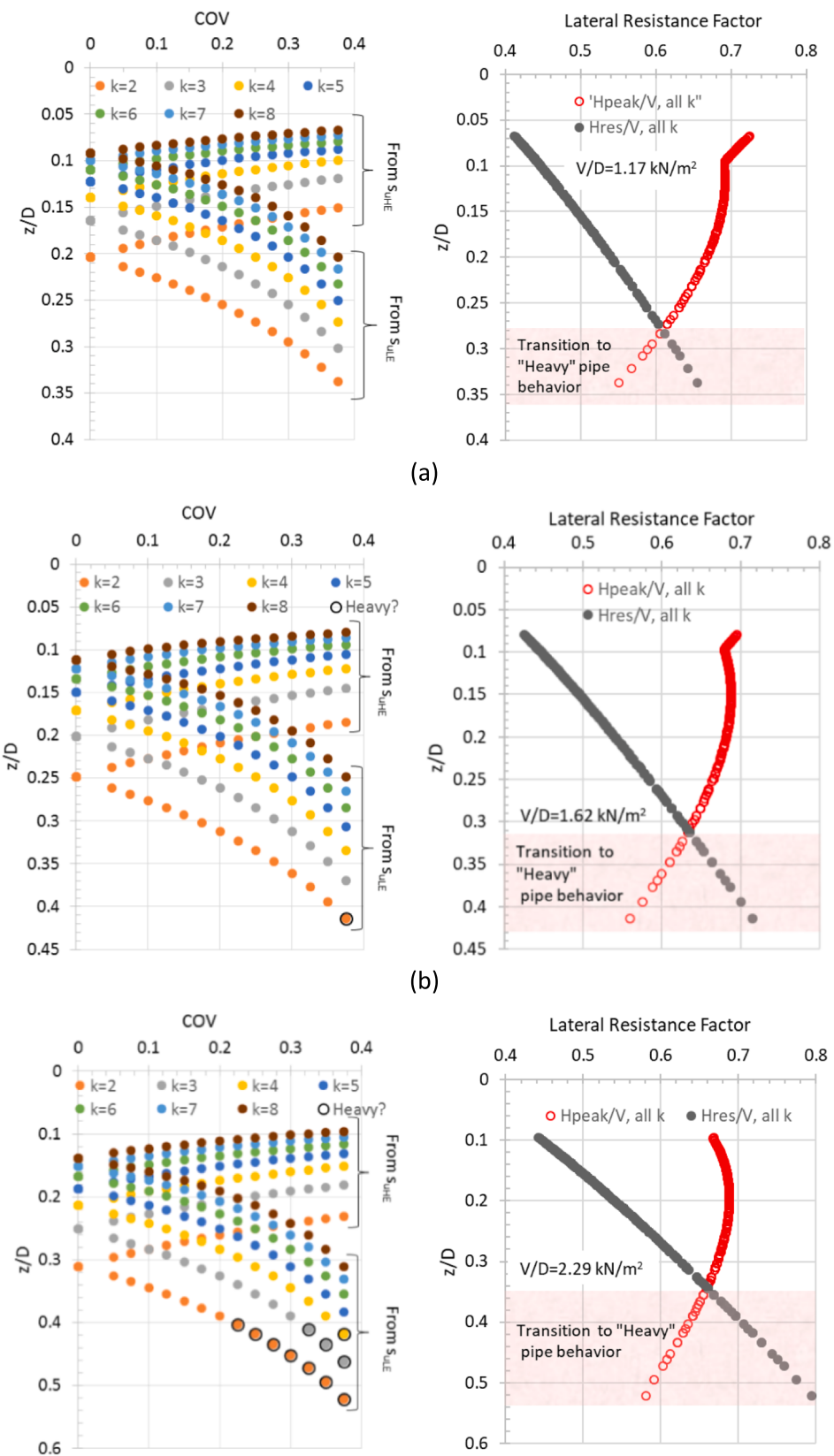
The residual lateral resistance ( $H_{res}/V$ ) shown in Eq. (13) is a function of normalized embedment only. It is shown as the grey line in the  $H/V$  vs  $z/D$  charts of Fig. 7, Fig. 8 and Fig. 9. The value of  $H_{res}/V$  which is reached only after a significant amount of lateral movement has occurred, is expected to be lower than the peak resistance ( $H_{peak}/V$ ) which is related to the breakout resistance when the pipeline first begins to move. In almost all of the lateral resistance factor versus embedment charts, the red curve (i.e.  $H_{peak}/V$ ) and the grey curve ( $H_{res}/V$ ) cross at a given embedment and the residual resistance becomes higher than the peak. The zone that is beneath this point of intersection has been shaded light pink and labeled as “Transition to “Heavy” pipe behavior”. “Heavy pipes” tend to embed further into the seabed as they are displaced laterally and, as a result, a limiting residual resistance may not be reached. It is noted that the database on which Eq. (13) is based does not include “Heavy” pipe behavior. T shaded zone draws attention to the possibility that “Heavy” pipe behavior may be possible be observed. In this study, the pipe weight is kept constant but as the COV increases, the  $s_{uLE}$  value and the related bearing capacity decreases such that the pipe, in effect, becomes “heavy” compared to the soil capacity.

A check for potential heavy pipe behavior was made for all pipe-soil strength combinations analyzed. Those combinations for which the pipe weight was more than half the bearing capacity of the soil at 50% embedment were identified. These combinations are indicated in Fig. 7 through Fig. 9 by a black circle around the data marker and have the series label “Heavy?”. The  $H_{res}/V$  values corresponding to these points should be viewed with added caution as this empirical model is not valid for pipes that show heavy pipe behavior. It is noted that in checking for heavy pipe behavior the lift force due to the buoyancy of the pipeline embedded in the soil has been taken into account by subtracting this value from the pipe submerged weight.

All pipe-soil combinations where heavy pipe behavior may potentially occur are noted to occur in low mean strength soils (i.e.  $k = 2, 3$  and 4 kPa) combined with a high COV value. The values of the LE shear strength,  $s_{uLE}$ , (Eq. (5)) for which potential heavy pipe behavior could occur (based on the bearing capacity criteria) were found to have  $k$  values that ranged from 0.5 kN/m<sup>2</sup>/m to 1.1 kN/m<sup>2</sup>/m for all three pipeline diameters analyzed.

In order to compare how each parameter of interest ( $z/D$ ,  $H_{peak}/s_{uD}$  and  $H_{res}/Ds_u$ ) changes with an increase in the variation of shear strength, or COV, the prediction interval lengths,  $PIL$ , were calculated. Fig. 10 shows an example for identifying the  $PILs$  for  $z/D$ ,  $H_{peak}$  and  $H_{res}$  parameters for a pipe of nominal stress 1.62 kN/m<sup>2</sup>, mean remolded shear strength gradient of 4 kPa/m and a COV of 30%. Following the blue arrows, the chart on the left shows the  $PIL$  for embedment and the chart on the right shows the  $PIL$  for peak and residual lateral resistance factors.

The values of  $PIL$  corresponding to COV of 0.1, 0.2, and 0.3 are presented in Figs. 11 to 13 for pipelines with diameters of 0.6 m, 0.8 m and 1.0 m respectively. In these figures the lengths of the bars are the

Fig. 7. Results for  $D = 0.6$  m and  $V/D$  of (a)  $1.17 \text{ kN/m}^2$  (b)  $1.62 \text{ kN/m}^2$  and (c)  $2.29 \text{ kN/m}^2$ .

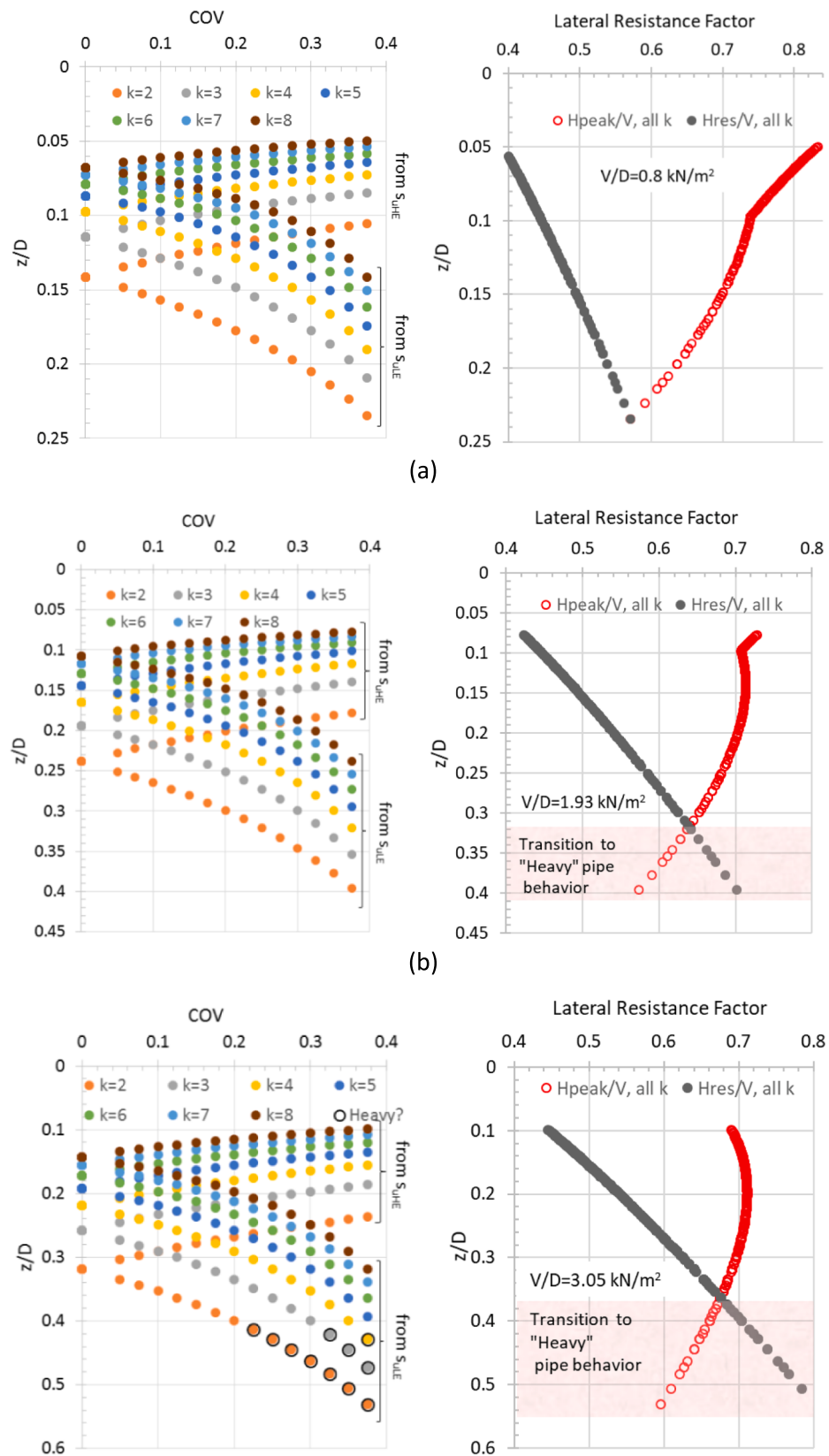


Fig. 8. Results for  $D = 0.8$  m and  $V/D$  of (a)  $0.80 \text{ kN/m}^2$  (b)  $1.93 \text{ kN/m}^2$  and (c)  $3.05 \text{ kN/m}^2$ .

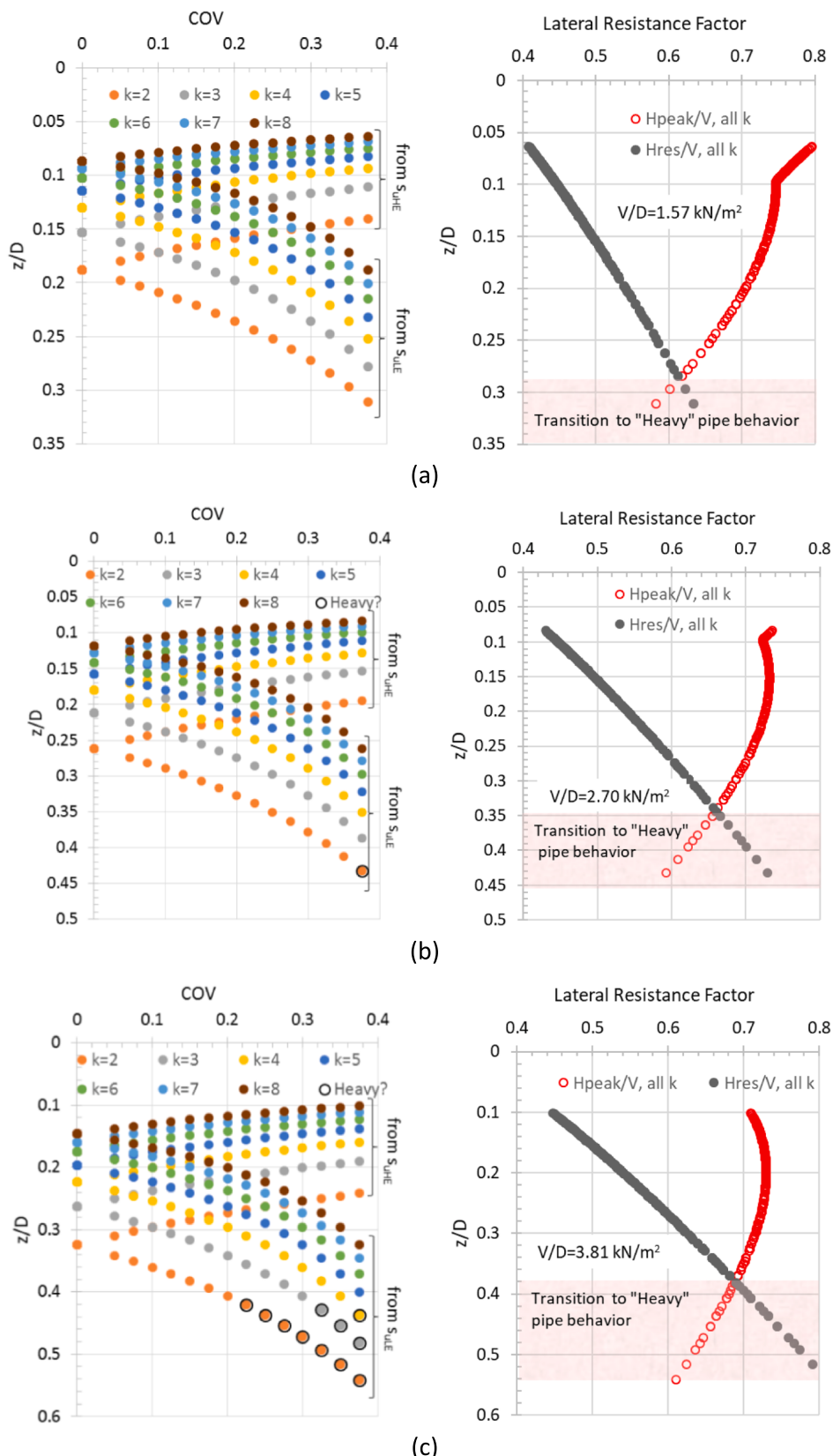
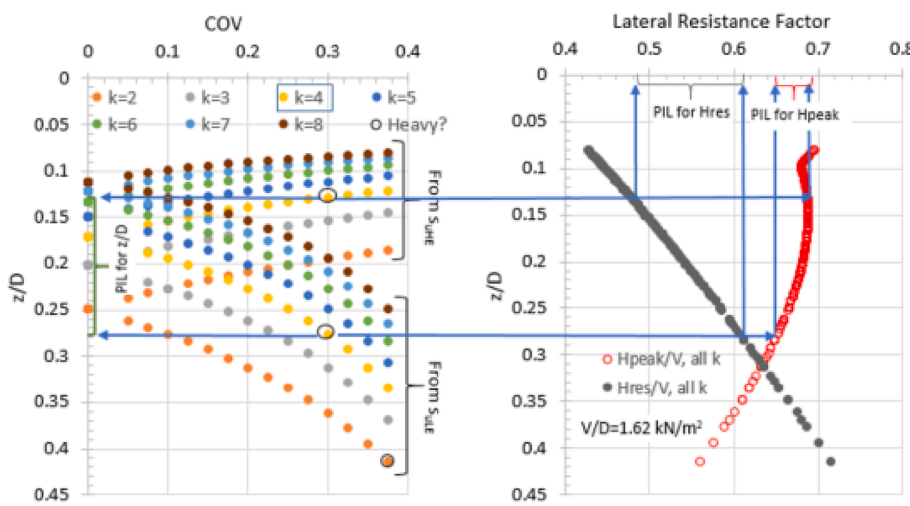


Fig. 9. Results for  $D = 1.0$  m and  $V/D$  of (a)  $1.57 \text{ kN/m}^2$  (b)  $2.70 \text{ kN/m}^2$  and (c)  $3.81 \text{ kN/m}^2$ .



**Fig. 10.** Example for identifying *PIL* values for  $D = 0.60$  m and  $V/D = 1.62$  kN/m and  $COV = 30\%$ .

prediction interval length, or *PIL*, for normalized embedment ( $z/D$ ), peak horizontal friction factor ( $H_{peak}/V$ ) and residual horizontal friction factor ( $H_{res}/V$ ). The same information is presented numerically in Tables 3 to 5.

It can be observed that for any given series consisting of a pipeline nominal weight ( $V/D$ ) and a mean  $k$  value, the *PIL* for normalized embedment increases with increasing *COV*. This is expected, and it indicates that the range of embedment values corresponding to variations in shear strength within a  $\pm 2\sigma$  band around the mean strength increases with increasing *COV*. Additionally, for any given *COV* value, the *PIL* value decreases with increasing value of mean  $k$ . This means that the range of embedment values becomes narrower as the mean shear strength of the soil increases. These two trends are consistent for all pipe weight-diameter combinations and mean soil strength gradients analyzed.

The *PIL* for normalized embedment also increases with increasing pipe nominal weight,  $V/D$ . This is true at all levels of shear strength variability, or *COV*. The *PIL* for residual horizontal friction factor follows the same trend since it is a function of only embedment. The *PIL* for peak horizontal friction factor decreases with increasing  $V/D$  for low mean strength gradients (i.e. 2 kPa/m, 3 kPa/m and 4 kPa/m). At higher mean shear strength gradients, lower embedment values occur which are in the proximity of local peak and/or discontinuity feature of the  $H_{peak}/V$  vs  $z/D$  curve. The proximity to this peak, tends to disrupt the above mentioned trend.

The  $H_{res}/V$  value is a function of only the normalized embedment. Hence, the changes in *PIL* for the residual horizontal resistance follows the same trend observed for *PIL* values for normalized embedment. The only difference is that the change in *PIL* for  $H_{res}/V$  value is of a smaller magnitude (i.e. the change is less steep) than the changes observed in *PIL* for  $z/D$ . Hence it may be stated that the range of  $H_{res}/V$  values corresponding to variations in shear strength within a  $\pm 2\sigma$  band around the mean strength increases with increasing *COV* and decreases with increasing mean strength.

The *PIL* values for  $H_{peak}/V$  follow a slightly different trend. The *PIL* value for  $H_{peak}/V$  tends to increase with increasing *COV* for most series of pipe and mean  $k$  value. Those series that deviate from this trend are those series with higher mean  $k$  values (i.e.  $k = 6, 7$ , and  $8$ ) which have best estimate normalized embedment, ( $z/D$ ), lower than 0.2. It can be seen that the  $H_{peak}/V$  vs  $z/D$  relationships shown by the red curves in Fig. 7 through Fig. 9 sometimes show a local peak at an embedment somewhere in the  $z/D$  range 0.1 to 0.2. This local peak and the low embedment associated with the higher mean  $k$  values disrupts the general trend of increasing *PIL* with increasing *COV*. It is noted however that the magnitude of change in *PIL* is fairly low in these cases.

The *PIL* values of  $H_{peak}/V$  at any selected *COV* show an initial downward trend followed by an upward trend with increasing mean  $k$  value. It has already been established that the variation in  $z/D$  decreases with increasing mean  $k$  and that the relationship between  $z/D$  and  $H_{peak}/V$  is non-linear with a local peak and a point of discontinuity at low embedment values. At higher mean  $k$  values (i.e.  $k$  equal to 6, 7 or 8 kN/m), the embedment is low enough to be in the proximity of these local features. This causes the  $H_{peak}/V$  prediction interval length to increase with further increases in the mean  $k$  value (for any constant *COV* value). The upward trend in the *PIL* is present but it is noted that the associated changes in magnitude are minor compared to those changes observed in the downward trend. This is because the lower mean  $k$  values tend to produce larger embedment variation compared to higher mean  $k$  values thus resulting in higher *PILs* for  $H_{peak}/V$ .

The top half meter of deep water seabed clays typically have undrained shear strengths that are in the range of a few kilopascals. These values correspond to the low mean  $k$  values (i.e.  $k$  equal to 2, 3 or 4 kN/m) used in this study. For clay soils with such low strength profiles, the  $H_{peak}/V$  parameter also increases with increasing *COV*. The prediction interval length for  $H_{peak}/V$  also decreases with increasing mean  $k$  value. For stiffer clay soils where the undrained shear strength gradient is  $>4$  kPa, the prediction interval length shows either a slow increase or remains virtually unchanged as the *COV* increases. Increases in the mean  $k$  value beyond 4 kPa do not impact the magnitude of *PIL* for  $H_{peak}/V$  significantly. This difference in impact is related to the very low normalized embedment associated with these higher strength clays and the non-uniform shape of the solution equations.

The LE and HE strength profiles were defined based on a mean value and a *COV* around the mean which corresponds to  $\pm 2$  standard deviations. Hence, the prediction interval lengths show the variation in design parameters caused by a strength range representing 95% of the shear strength distribution. Evaluation of the result from this study show the following findings.

- **Embedment:** For a constant *COV* value, the prediction interval length decreases as the mean shear strength of the soil increases. This means that the range of embedment values becomes narrower as the mean strength increases.
- **Peak lateral friction factor,  $H_{peak}/V$ :** For clay soils with strength profiles lower than 4 kPa, the prediction interval length increases with increasing *COV* strength and decreases with increasing mean  $k$  value.
- **Peak lateral friction factor,  $H_{peak}/V$ :** For stiffer clay soils where undrained shear strength is  $>4$  kPa, the prediction interval length shows either a slow increase or remains virtually unchanged as the *COV*

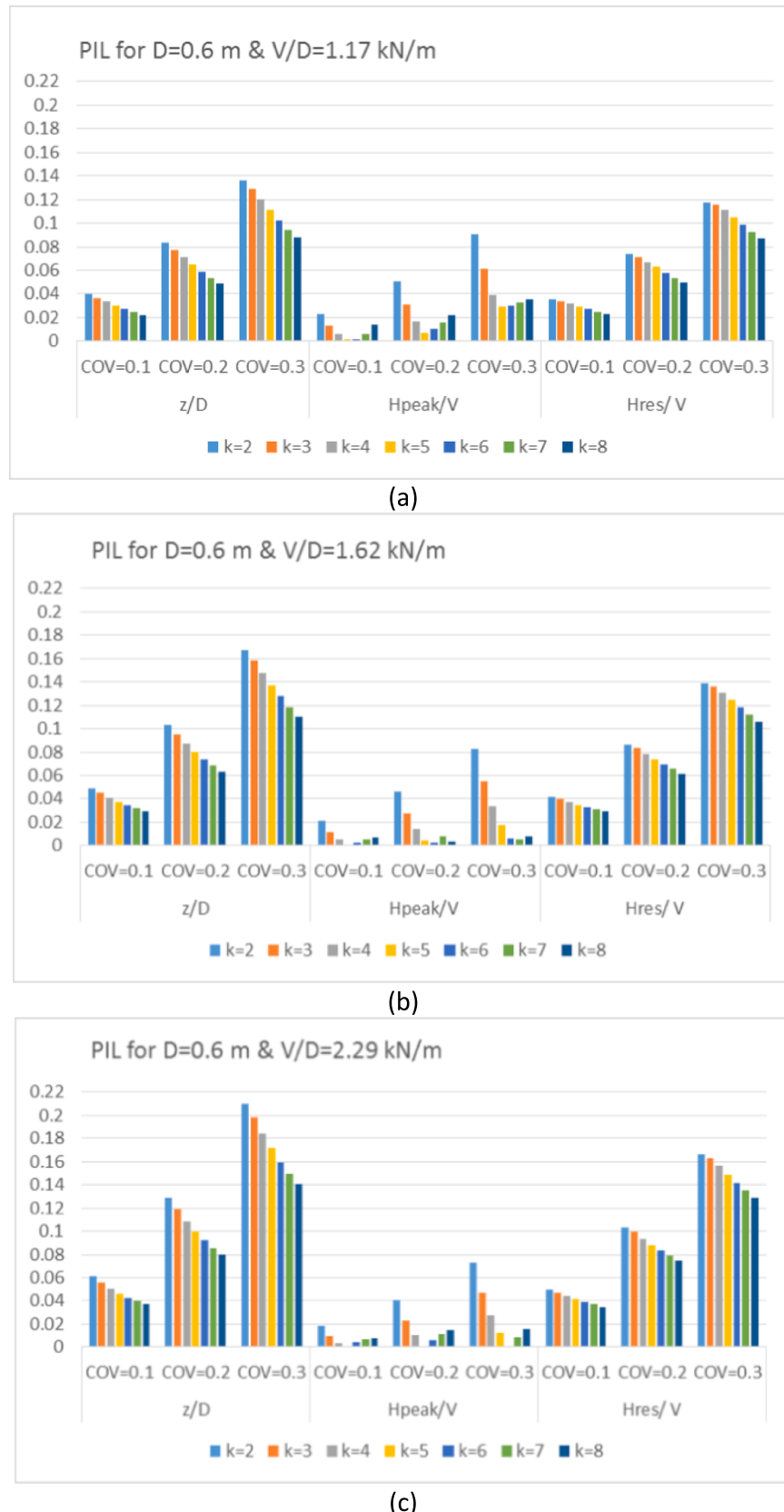


**Fig. 11.** Prediction interval lengths for  $D = 0.60 \text{ m}$  and  $V/D$  equal to (a)  $1.17 \text{ kN/m}^2$  (b)  $1.62 \text{ kN/m}^2$  and (c)  $2.29 \text{ kN/m}^2$ .

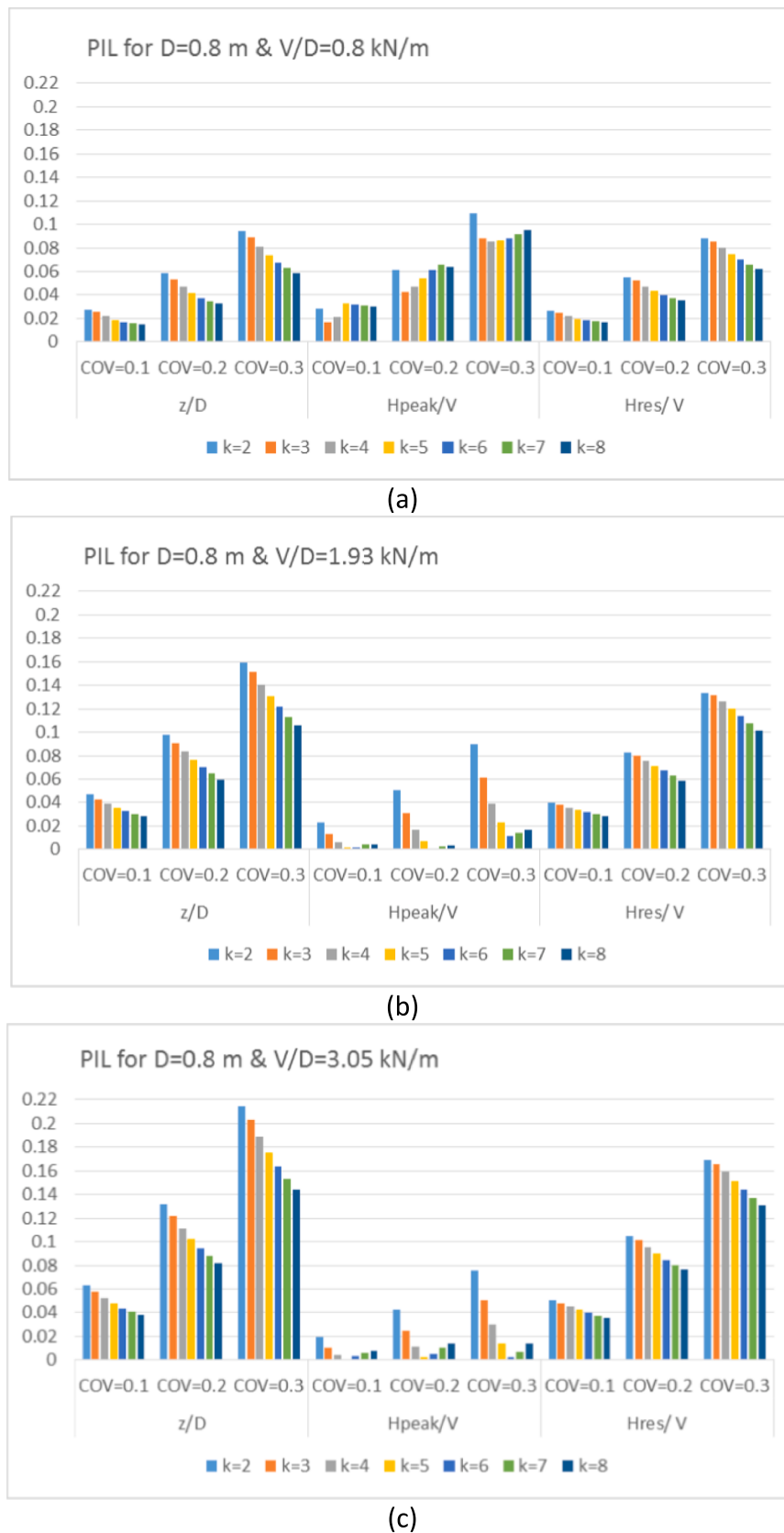


**Fig. 12.** Prediction interval lengths for  $D = 0.80 \text{ m}$  and  $V/D$  equal to (a)  $0.8 \text{ kN/m}^2$  (b)  $1.93 \text{ kN/m}^2$  and (c)  $3.05 \text{ kN/m}^2$ .

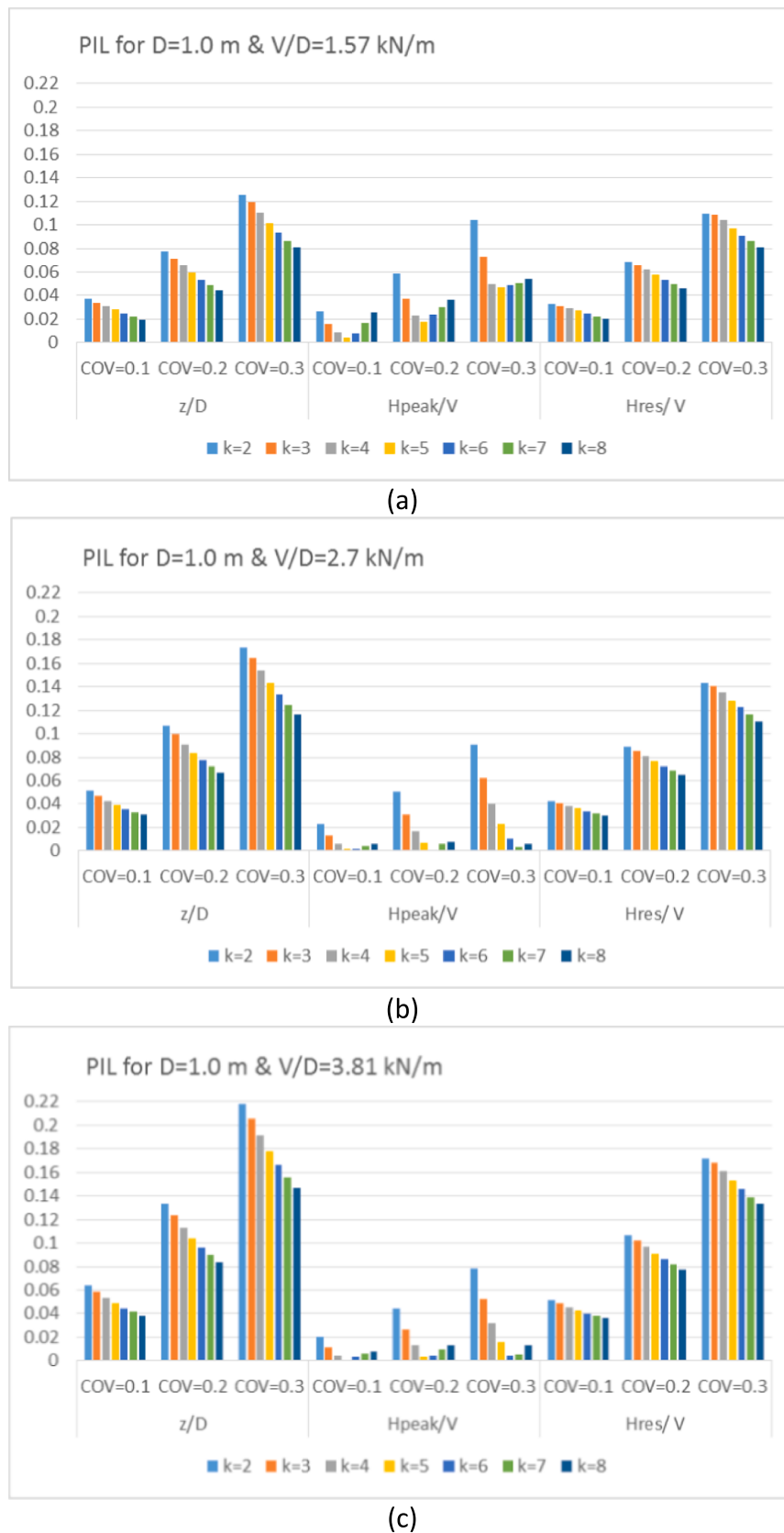


**Fig. 13.** Prediction interval lengths for  $D = 1.0 \text{ m}$  and  $V/D$  equal to (a)  $1.57 \text{ kN/m}^2$  (b)  $2.7 \text{ kN/m}^2$  and (c)  $3.81 \text{ kN/m}^2$ .

**Table 3**Prediction Interval Lengths for  $D = 0.60$  m pipeline.

k kPa/m	COV	$V/D = 1.17 \text{ kN/m}^2$			$V/D = 1.62 \text{ kN/m}^2$			$V/D = 2.29 \text{ kN/m}^2$		
		Z/D	H <sub>peak/V</sub>	H <sub>res/V</sub>	Z/D	H <sub>peak/V</sub>	H <sub>res/V</sub>	Z/D	H <sub>peak/V</sub>	H <sub>res/V</sub>
2	0.1	0.040	0.023	0.035	0.049	0.021	0.042	0.062	0.019	0.050
	0.2	0.084	0.051	0.073	0.103	0.046	0.086	0.129	0.041	0.103
	0.3	0.136	0.090	0.118	0.167	0.083	0.139	0.210	0.073	0.167
3	0.1	0.037	0.013	0.034	0.045	0.012	0.040	0.056	0.010	0.047
	0.2	0.078	0.031	0.071	0.095	0.027	0.083	0.119	0.023	0.099
	0.3	0.129	0.061	0.116	0.158	0.055	0.136	0.198	0.047	0.163
4	0.1	0.033	0.006	0.032	0.041	0.005	0.037	0.051	0.003	0.044
	0.2	0.071	0.017	0.067	0.087	0.014	0.078	0.109	0.010	0.094
	0.3	0.120	0.039	0.111	0.148	0.034	0.131	0.184	0.027	0.156
5	0.1	0.030	0.002	0.030	0.037	0.000	0.035	0.047	0.001	0.042
	0.2	0.065	0.007	0.063	0.080	0.004	0.074	0.100	0.001	0.088
	0.3	0.111	0.030	0.105	0.137	0.018	0.124	0.171	0.012	0.149
6	0.1	0.028	0.001	0.028	0.034	0.003	0.033	0.043	0.004	0.039
	0.2	0.059	0.010	0.058	0.074	0.003	0.070	0.092	0.006	0.083
	0.3	0.102	0.030	0.098	0.128	0.006	0.118	0.160	0.000	0.142
7	0.1	0.025	0.006	0.025	0.032	0.005	0.031	0.040	0.007	0.037
	0.2	0.054	0.016	0.054	0.069	0.008	0.066	0.086	0.011	0.079
	0.3	0.095	0.032	0.093	0.119	0.006	0.112	0.150	0.009	0.135
8	0.1	0.022	0.014	0.023	0.030	0.007	0.029	0.037	0.008	0.035
	0.2	0.049	0.022	0.050	0.063	0.003	0.062	0.080	0.015	0.075
	0.3	0.088	0.035	0.088	0.111	0.008	0.106	0.141	0.016	0.129

**Table 4**Prediction Interval Lengths for  $D = 0.80$  m pipeline.

k kPa/m	COV	$V/D = 0.8 \text{ kN/m}^2$			$V/D = 1.93 \text{ kN/m}^2$			$V/D = 3.05 \text{ kN/m}^2$		
		Z/D	H <sub>peak/V</sub>	H <sub>res/V</sub>	Z/D	H <sub>peak/V</sub>	H <sub>res/V</sub>	Z/D	H <sub>peak/V</sub>	H <sub>res/V</sub>
2	0.1	0.028	0.028	0.026	0.047	0.023	0.040	0.063	0.019	0.050
	0.2	0.058	0.061	0.055	0.098	0.051	0.083	0.132	0.043	0.105
	0.3	0.095	0.109	0.088	0.159	0.090	0.133	0.214	0.076	0.169
3	0.1	0.025	0.017	0.025	0.043	0.013	0.038	0.057	0.010	0.048
	0.2	0.054	0.042	0.052	0.091	0.031	0.080	0.122	0.025	0.101
	0.3	0.089	0.088	0.085	0.151	0.061	0.131	0.203	0.050	0.166
4	0.1	0.022	0.021	0.022	0.039	0.006	0.036	0.052	0.004	0.045
	0.2	0.047	0.047	0.047	0.083	0.017	0.076	0.111	0.012	0.095
	0.3	0.081	0.086	0.080	0.141	0.039	0.126	0.188	0.030	0.159
5	0.1	0.019	0.033	0.019	0.036	0.002	0.034	0.048	0.000	0.042
	0.2	0.042	0.054	0.043	0.077	0.007	0.071	0.102	0.002	0.090
	0.3	0.074	0.086	0.074	0.131	0.023	0.120	0.175	0.014	0.151
6	0.1	0.017	0.032	0.018	0.033	0.002	0.031	0.044	0.004	0.040
	0.2	0.038	0.061	0.040	0.071	0.000	0.067	0.094	0.005	0.085
	0.3	0.068	0.088	0.070	0.122	0.012	0.114	0.163	0.002	0.144
7	0.1	0.016	0.031	0.017	0.030	0.004	0.030	0.041	0.006	0.038
	0.2	0.035	0.066	0.037	0.065	0.003	0.063	0.088	0.010	0.080
	0.3	0.063	0.091	0.066	0.113	0.014	0.107	0.153	0.007	0.137
8	0.1	0.015	0.030	0.016	0.028	0.004	0.028	0.038	0.008	0.036
	0.2	0.033	0.064	0.035	0.060	0.003	0.059	0.082	0.014	0.076
	0.3	0.058	0.095	0.062	0.105	0.016	0.101	0.144	0.014	0.131

increases. Increases in the mean  $k$  value beyond 4 kPa do not impact the magnitude of PIL significantly.

- **Residual lateral friction factor,  $H_{\text{res}/V}$ :** For a given pipe geometry, the prediction interval length increases with increasing COV and decreases with increasing mean  $k$  value. This trend is similar to the trend in embedment.

## 6. Discussion

The embedment of on-bottom subsea pipelines installed in deep water clay seabed is a complex geotechnical problem influenced by many parameters including the installation water depth, lay conditions (i.e. sea state), pipeline stiffness and weight, soil stiffness and stress concentrations at the touchdown point. This makes it difficult to readily identify how shear strength variability impacts design variables such as the horizontal peak and residual resistances and the respective friction factors.

The buckling of deep water HPHT pipelines is greatly impacted by the mobilized shearing resistance of seabed clays in the top half meter of the seabed. Typically, these clays have low shear strength. Sampling and testing at intervals along a pipeline route can provide data for estimating the inherent variability that exists along that route. In PSI studies the embedment and friction factors (axial and lateral) for a given pipe-soil combination are evaluated. Typically, variability in shear strength is taken into account by conducting additional analyses using LE and HE strength profiles with the corresponding PSI parameters also labeled as LE and HE values. However, this approach can lead to an over- or underestimation of the range of PSI parameters. It has been demonstrated that calculations combining simultaneous onerous extreme values of input parameters tend to produce PSI parameter limits that are widely varied (yet extremely unlikely) which can lead to overly conservative design solutions [32].

The COV of undrained shear strength, as reported in laboratory tests, was shown to range from 6% to 80% with a mean value of 32% [21]. The

**Table 5**  
Prediction Interval Lengths for  $D = 1.00$  m pipeline.

k kPa/m	COV	$V/D = 1.57 \text{ kN/m}^2$			$V/D = 2.70 \text{ kN/m}^2$			$V/D = 3.81 \text{ kN/m}^2$		
		Z/D	$H_{\text{peak}}/V$	$H_{\text{res}}/V$	Z/D	$H_{\text{peak}}/V$	$H_{\text{res}}/V$	Z/D	$H_{\text{peak}}/V$	$H_{\text{res}}/V$
2	0.1	0.037	0.027	0.033	0.051	0.023	0.043	0.064	0.020	0.051
	0.2	0.077	0.059	0.068	0.107	0.051	0.089	0.134	0.045	0.106
	0.3	0.125	0.104	0.110	0.174	0.090	0.143	0.218	0.078	0.171
3	0.1	0.034	0.016	0.031	0.047	0.013	0.041	0.058	0.011	0.049
	0.2	0.071	0.038	0.066	0.099	0.031	0.086	0.124	0.026	0.102
	0.3	0.119	0.073	0.108	0.165	0.062	0.141	0.206	0.053	0.168
4	0.1	0.031	0.009	0.029	0.043	0.006	0.038	0.053	0.005	0.046
	0.2	0.065	0.023	0.062	0.091	0.017	0.081	0.113	0.013	0.097
	0.3	0.111	0.049	0.104	0.154	0.040	0.135	0.192	0.032	0.161
5	0.1	0.028	0.004	0.028	0.039	0.002	0.036	0.048	0.000	0.043
	0.2	0.060	0.017	0.058	0.084	0.007	0.076	0.104	0.003	0.091
	0.3	0.101	0.047	0.097	0.143	0.023	0.129	0.178	0.016	0.153
6	0.1	0.025	0.008	0.025	0.036	0.002	0.034	0.045	0.003	0.040
	0.2	0.054	0.024	0.053	0.077	0.000	0.072	0.096	0.004	0.086
	0.3	0.093	0.049	0.091	0.134	0.010	0.122	0.166	0.004	0.146
7	0.1	0.022	0.017	0.023	0.033	0.004	0.032	0.041	0.006	0.038
	0.2	0.049	0.030	0.049	0.072	0.006	0.068	0.089	0.009	0.081
	0.3	0.087	0.051	0.086	0.125	0.003	0.116	0.156	0.005	0.139
8	0.1	0.020	0.026	0.020	0.031	0.006	0.030	0.039	0.008	0.036
	0.2	0.045	0.037	0.046	0.067	0.008	0.065	0.084	0.014	0.077
	0.3	0.081	0.054	0.081	0.116	0.006	0.110	0.147	0.013	0.133

inherent variability in terms of COV of undrained shear strength, as measured in field vane shear tests, was shown to range from 4% to 44% with a mean value of 24% [20]. The typical range of variability for undrained shear strength obtained from good-quality direct laboratory or field measurements was reported to range from 10 to 30% COV (considered low variability) [19]. The COV values used in this study range from 5% to 37.5%. This range encompasses, to a large extent, the above reported inherent variability of undrained shear strength of clays as measured in laboratory and field tests.

Alternatives to this deterministic approach are the use of probabilistic methods such as the Monte Carlo-based simulation approach [14,15,25,32] which provide a more rigorous way to handle the uncertainty. In the probabilistic methods the input variables are treated as random variables with statistical distributions. Any identified correlation between input variables may also be incorporated in the calculation.

Both deterministic and probabilistic approaches require an efficient calculation method to evaluate the breakout and residual resistances for the relevant combinations of pipeline embedment, relevant pipeline weight at the time of movement (i.e. water- or product-filled) and seabed geotechnical properties. The charts developed in this study allow for a visual assessment of the impact of COV in strength on the lateral friction factors. They may be used in a qualitative assessment of strength variability on peak and residual friction factors for pipelines with diameters ranging from 0.6 to 1.0 m and  $V/D$  ratios ranging from 0.8 to 3.05  $\text{kN/m}^2$ . The PSI-Lateral code may be used to develop project specific charts for making quantitative assessments. The PSI-Lateral code may also be incorporated in Monte Carlo analyses for probabilistic assessments of global buckling or used as a research tool for other pipeline related studies.

## 7. Conclusions

In PSI analysis the associated best practice solution methods involve many parameters, are implicit and non-linear in nature making it difficult to readily understand the impact of strength variability on the design parameters such as  $H_{\text{peak}}/V$  and  $H_{\text{res}}/V$ . A calculation tool, 'PSI - Lateral', has been written in the R programming language to evaluate the embedment and corresponding lateral resistances (peak and residual) for pipeline geometries defined by a diameter and wall thickness and any remolded strength profile defined by a linearly increasing shear strength profile. PSI-Lateral takes into account many associated design

parameters and follows the state-of-the-art recommended procedure in industry guidelines. This code has been used to conduct a parametric analysis for determining the influence of the variability of undrained shear strength (expressed by the COV) on the embedment and the peak and residual friction factors ( $H_{\text{peak}}/V$  and  $H_{\text{res}}/V$ ) of on-bottom subsea pipelines. Three selected pipeline diameters and 9 pipeline nominal weights were evaluated to determine the prediction interval lengths of the three design parameters ( $z/D$ ,  $H_{\text{peak}}/V$  and  $H_{\text{res}}/V$ ) for mean shear strength gradients varying from 2 to 8 kPa/m and COV ranging from 5% to 37.5%. The parametric study conducted and the charts developed allow a systematic (and visual) evaluation of how changes in mean shear strength and COV impact the design variables.

For the range of pipe-soil combinations considered in this study, the findings may be summarized as follows:

- Expected range of normalized embedment ( $z/D$ ): It increases with increasing COV and decreases with increasing mean shear strength  $k$  for all pipelines tested.
- Expected range of horizontal peak resistance factor ( $H_{\text{peak}}/V$ ): It increases with increasing COV and decreases with increasing mean  $k$  value for clay soils with mean shear strength profiles lower than 4 kPa/m. For clay soils with mean shear strengths > 4 kPa/m, the range of expected  $H_{\text{peak}}/V$  values is both low and mostly insensitive to increases in COV and increases in mean  $k$  value unless the pipeline is very light in which case there are small increases associated with increasing  $k$  and COV.
- Expected range of horizontal residual resistance factor ( $H_{\text{res}}/V$ ): It increases with increasing COV and decreases with increasing mean shear strength  $k$  for all pipelines tested.

The charts developed may be used directly to estimate appropriate ranges for design parameters for pipelines with nominal stresses on soil ( $W'/D$ ) that are in the range of 0.8 to 3.05  $\text{kN/m}^2$ . Alternately, the PSI-Lateral code may be used to conduct similar analyses for project specific or research oriented studies.

## Declaration of Competing Interest

The authors declare that they have no known competing financial interests or personal relationships that could have appeared to influence the work reported in this paper.

## Appendix:. Listing of R code “PSI-Lateral”

```

#SL = Residual lay tension (horizontal component of lay tension) (in
kN)
#Do = Overall coated outside diameter (nominal) (in m)
#Di = Internal diameter (nominal) (in m)
#Ts = Steel thickness (in m)
#Es = Steel modulus of elasticity (in kPa)
#Is = Second Moment of Inertia of combined steel cross-section (in
cm^4)
#wi = Pipe submerged weight at installation (empty) (in kN/m)
#wp = Pipe submerged weight at operation (in kN/m)
#Su = Undisturbed undrained shear strength entered as slope and
intercept (in kPa)
#Sur = Remolded undrained shear strength entered as slope and
intercept (in kPa)
#SUW = Soil submerged unit weight entered as a constant (in kN/
m^3)
#OCR = Overconsolidation ratio (ratio of maximum pipe weight to
current pipe weight)
#zw = water depth (in m)
#Fu_LBOU = Undrained lateral breakout resistance (in kN/m)
# Fu_LresU = Undrained lateral residual resistance (in kN/m)
#Abm is the submerged area of pipe (in m^2)
rm(list = ls())
Abm <- function(z,Do) {
  if (z/Do > 1)
    {pi*Do^2/4}
  else{Do^2/4*(acos(1-2*z/Do)-sin(acos(1-2*z/Do))*(1-2*z/Do))}
}
Sur_approx <- function(z, Sum, k){Sum + k*z}
Su_approx <- function(z,Su0,k0){Su0 + k0*z}
Klay1 <- function(z, Do,wi, Sum, k, SUW) {
  6*(z/Do)^0.25*Do*(Sur_approx(z, Sum, k)/wi) + 1.5*SUW*Abm(z,
Do)/wi}
Klay2 <- function(z, Do,wi,Sum, k, SUW) {
  3.4*sqrt(10*z/Do)*(Sur_approx(z, Sum, k)*Do/wi) +
  1.5*SUW*Abm(z, Do)/wi
}
KlayB45<- function(z, Do,wi,Sum,k, SUW) {
  Kl1 <- -Klay1(z,Do,wi,Sum,k, SUW)
  Kl2 <- -Klay2(z,Do,wi,Sum,k, SUW)
  if(Kl1 < Kl2)
    Kl1
  else
    Kl2
}
KlayOD <- function(z,Do,wi,Sum,k, SUW) {
  6*(z/Do)^0.25*Do*(Sur_approx(z, Sum, k)/wi) + 1.5*SUW*-
  Do^2*pi/(4*wi)
}
KlayB45i <- function(z,Do,wi,Sum,k, SUW) {
  if (z/Do > 1){ KlayOD(z,Do,wi,Sum,k, SUW)}
  else{KlayB45(z,Do,wi,Sum,k, SUW)}
}
So <- function(Es,Is,wi){(3*sqrt(Es*Is)*wi)^(2/3)}
KlayB47i<- function(z,Do,wi,Es,Is,SL,Sum,k, SUW){
  Es <- -Es
  Is <- -Is
  0.6 + 0.4*(Es*Is*KlayB45i(z,Do,wi,Sum,k, SUW)*wi/(z*SL^2))^0.25
}
bisect <- function(fn,min,max){
  if(fn(min)*fn(max) > 0)
    print("cannot continue in bisect\n")
  a < -min
  b < -max
}

```

```

while (b-a > 1e-8){
  c<-(a + b)/2
  if (fn(a)*fn(c) > 0) {a < -c}
  else {b < -c}
}
c
}
solve_KlayB47i_minus_KLayB45i <- -function(Do,wi,Es,Is,SL,min,
max,Sum,k,SUW){
  f <- function(z){
    KlayB47i(z,Do,wi,Es,Is,SL,Sum,k, SUW)-KlayB45i(z,Do,wi,Sum,k,
SUW)
  }
  bisect(f,min,max)
}
solve_1_minus_KlayB45 <- function(Do,wi,min,max,Sum,k,SUW){
  f <- function(z){
    1-KlayB45(z,Do,wi,Sum,k, SUW)
  }
  bisect(f,min,max)
}
thetaw <- function(z,Do){
  min(pi/2,acos(1-2*min(1,z/Do)))
}
Xi <- function(z,Do){
  th <- -thetaw(z,Do)
  if(th>=pi/2){ 2*sin(pi/2)/(pi/2 + sin(pi/2)*cos(pi/2))}
  else{ 2*sin(th)/(th + sin(th)*cos(th))}
}
li2 <- function(z,Do){
  if(z > Do){pi*Do}
  else{Do*acos(1-2*z/Do)}
}
Fu_LBOU <- function(z, Do, wp,Su0, k0){
  (1.7*(z/Do)^0.61 + 0.23*(wp/(Do*Su0))^(0.83+0.6*(SUW*Do/Su0))^(z/Do)^2)*Do*Su0
}
Fu_LresU <- function(z, Do){
  (0.32 + 0.8*(z/Do)^0.8)*wi
}
#function definitions end here
names<- c("Estimate","SUW","Ts","wi","Do","Sum","k","c","SL",
"Is","Es","Su_Sur_ratio","klayz","Su_invert","Fu_LBOU","Fu_LresU",
"wi_Dsuave")
df <- data.frame()
for (j in names) df[[j]] <- as.numeric()
Su_invert <- 1
SL <- -1800
Su_Sur_ratio <- 3
Es <- -200*10^6
Is <- -880500*10^-8
Ts_index <- -c(0.036,0.04,0.045,0.050,0.055)
Sum_index <- -c(0)
k_index <- -c(2,3,4,5,6,7,8)
SUW_index <- -c(4)
Do_index <- -c(1.00)
wi_add <- 0
zw <- 2000
estim_type_index <- -c("LE","BE","HE")
cov_index <- -c(0.05,0.075,0.1,0.125,0.15,0.175,0.2,0.225,
0.25,0.275,0.3,0.325,0.35,0.375)
for(SUW in SUW_index){
  for(Do in Do_index){
    for(Ts in Ts_index){
      for(Sum in Sum_index){
        
```

```

for(k in k_index){
for(cov in cov_index){
for(estim_type in estim_type_index){
c < -cov*k
Di < -Do-2*Ts
Is < -pi*(Do^4-Di^4)/64
wi_air<-(pi/4)*(Do^2-Di^2)*8*9.81
wi_wtr<-(pi/4)*(Do^2)*1.025*9.81
wi < -wi_air-wi_wtr + wi_add
SL < -zw*wi*0.5198034
if (So(Es,Is,wi)>=SL){
print("cannot continue, increase SL")
#note that the coefficient 0.5198034 corresponds to pipe hangoff
angle of 70 degrees
orig_k < -k
if(estim_type=="LE")
k < -k-2*c
else if(estim_type=="HE")
k < -k + 2*c #if BE k remains the same
klayz < -solve_KlayB47i_minus_KLayB45i(Do,wi,Es,Is,SL,1e-5,2*Do,
Sum, k, SUW)
if(KlayB45i(klayz,Do,wi,Sum, k, SUW) less than 1){
klayz < -solve_1_minus_KlayB45(Do,wi,1e-5,2*Do,Sum, k, SUW)
}
Su_invert < -Su_approx(klayz,Sum,k)
Fu_LBOUval < -Fu_LBOU(klayz, Do, wi,Sum*Su_Sur_ratio,
k*Su_Sur_ratio)
Fu_LresUval < -Fu_LresU(klayz, Do)
wi_Dsuave<-(wi-SUW*pi*(Do^2)/8)/(Do*(Sur_approx(Do/2,Sum,k)
+ Sur_approx(3*Do/2,Sum,k))/2)
new_row = data.frame(Estimate = estim_type,SUW = SUW,Ts = Ts,
wi = wi,Do = Do,Sum = Sum,k = k, c = c, SL = SL, Is = Is, Es = Es,
Su_Sur_ratio = Su_Sur_ratio,klayz = klayz, Su_invert = Su_invert,Fu_L-
BOU = Fu_LBOUval,Fu_LresU = Fu_LresUval, wi_Dsuave = wi_Dsuave)
df < -rbind(df,new_row)
k < -orig_k
}}}}}}}
write.csv(df, file = 'C:/filename.csv')#use any folder/file name

```

## References

- [1] Api-rp-2geo, Geotechnical and foundation design considerations 1st ed., 2014 Addendum 1.
- [2] C.P. Aubeny, H. Shi, J.D. Murff, Collapse loads for a cylinder embedded in trench in cohesive soil, *Int. J. Geomech.* 5 (4) (2005) 320–325.
- [3] Bruton, D., White, D., Cheuk, C., Bolton, M., Carr, M., 2006. Pipe/soil interaction behavior during lateral buckling, including large-amplitude cyclic displacement tests by the safebuck JIP, in: OTC 17944. Presented at the Offshore Technology Conference, OnePetro, Houston, Texas.
- [4] D.A. Bruton Advances in Predicting Pipeline Embedment Based on Assessment of Field Data. Presented at the Offshore Technology Conference 2014 OnePetro.
- [5] D.A.S. Bruton, M. Carr, D. White, The influence of pipe-soil interaction on lateral buckling and walking of pipelines: the SAFEBUCK JIP, in: Presented at the Proc. 6th Int. Conf. on Offshore Site Investigation and Geotechnics, 2007, pp. 133–150.
- [6] C.O. Cardoso R. Silveira Pipe-soil interaction behavior for pipelines under large displacements on clay soils-A model for lateral residual friction factor, in: OTC 20767 2010 Houston, Texas.
- [7] S. Chatterjee, M.F. Randolph, D.J. White, The effects of penetration rate and strain softening on the vertical penetration resistance of seabed pipelines, *Géotechnique* 62 (7) (2012) 573–582.
- [8] H. Dendani, C. Jaek, Flowline and riser: Soil interaction in plastic clays. Presented at the Offshore Technology Conference, 2008.
- [9] H.R.C. Dingle, D.J. White, C. Gaudin, Mechanisms of pipe embedment and lateral breakout on soft clay, *Can. Geotech. J.* 45 (5) (2008) 636–652.
- [10] Dnv-rp-f110,, Global Buckling of Submarine Pipelines due to High Temperature and Pressure, Det Norske Veritas, 2017.
- [11] Dnv-rp-f114,, Pipe-soil interaction for submarine pipelines, No. DNV-RP-F114, Det Norske Veritas, 2017.
- [12] W. Dunlap R. Bhojanala D. Morris Burial of vertically loaded offshore pipelines in weak sediments 1990 Houston, Texas.
- [13] C.M. Martin, D.J. White, Limit analysis of the undrained bearing capacity of offshore pipelines, *Géotechnique* 62 (9) (2012) 847–863.
- [14] W. McCarron Limit analysis and finite element evaluation of lateral pipe-soil interaction resistance Canadian geotechnical journal 53 2016 14 21 https://doi.org/10.1139/cj-2014-0409.
- [15] W. McCarron, Subsea flowline buckle capacity considering uncertainty in pipe-soil interaction, *Comput. Geotech.* 68 (2015) 17–27.
- [16] R.S. Merifield, D.J. White, M.F. Randolph, Effect of surface heave on response of partially embedded pipelines on clay, *J. Geotech. Geoenviron. Eng.* 135 (6) (2009) 819–829.
- [17] Merifield, R., White, D., Randolph, M., 2008. The effect of pipe-soil interface conditions on the undrained breakout resistance of partially-embedded pipelines.
- [18] J.D. Murff, D.A. Wagner, M.F. Randolph, Pipe penetration in cohesive soil, *Pipe penetration in cohesive soil. Géotechnique* 39 (2) (1989) 213–229.
- [19] Phoon, K.-K., Kulhawy, F.H., 2008. Serviceability limit state reliability-based design, in: Reliability-Based Design in Geotechnical Engineering. CRC Press, pp. 356–396.
- [20] K.-K. Phoon, F.H. Kulhawy, Characterization of geotechnical variability, *Can. Geotech. J.* 36 (4) (1999) 612–624.
- [21] K.-K. Phoon, F.H. Kulhawy, M.D. Grigoriu, Reliability based design of foundations for transmission line structures, No. TR-105000, Electric Power Research Institute, Palo Alto, 1995.
- [22] M. Randolph, S. Gourvenec, Offshore Geotechnical Engineering, 1st ed., Spon Press, New York, 2011.
- [23] M.F. Randolph D. White Pipeline embedment in deep water: processes and quantitative assessment. Presented at the Offshore Technology Conference 2008 OnePetro.
- [24] F. Sahdi J. Tom P. Watson C. Gaudin M. Bransby Effect of water entrainment on seabed soils during cyclic pipe-soil interaction 2020 AA Balkema Leiden, Netherlands.
- [25] C. Sicilia, P. Cooper, E. Bonnet, Probabilistic lateral buckling assessment, *IJOPE* 25 (4) (2015).
- [26] R. Verley, K. Lund, A soil resistance model for pipelines placed on clay soils, *American Society of Mechanical Engineers, New York, NY (United States), Presented at the Offshore Mechanics and Arctic Engineering, 1995*, pp. 225–232.
- [27] Wagner, D., Murff, J., Brennolden, H., Sveggen, O., 1987. Pipe-soil interaction model. Presented at the Annual Offshore Technology Conference. 19, OnePetro, Houston, Texas, pp. 181–190.
- [28] D. Wang, D.J. White, M.F. Randolph, Large-deformation finite element analysis of pipe penetration and large-amplitude lateral displacement, *Can. Geotech. J.* 47 (8) (2010) 842–856.
- [29] Z. Westgate, D. White, M. Randolph, Video observations of dynamic embedment during pipelaying in soft clay, Presented at the International Conference on Offshore Mechanics and Arctic Engineering (2009) 699–707.
- [30] Z. Westgate, D. White, M.F. Randolph, P. Brunning, Pipeline laying and embedment in soft fine-grained soils. Field Observations and Numerical Simulations. Presented at the Offshore Technology Conference, 2010.
- [31] Z.J. Westgate, W. Haneberg, D.J. White, Modelling spatial variability in as-laid embedment for high pressure and high temperature (HPHT) pipeline design, *Can. Geotech. J.* 53 (11) (2016) 1853–1865.
- [32] D. White, D. Cathie, Geotechnics for subsea pipelines, *Front. Offshore Geotechnics II* 1 (2011) 87–123.
- [33] D. White, E. Clukey, M. Randolph, N. Boylan, M. Bransby, A. Zakeri, A. Hill, C. Jaek, The state of knowledge of pipe-soil interaction for on-bottom pipeline design. Presented at the Offshore Technology Conference, 2017.
- [34] D.J. White, H.R.C. Dingle, The mechanism of steady friction between seabed pipelines and clay soils, *Géotechnique* 61 (12) (2011) 1035–1041.
- [35] D. White Z. Westgate J. Ballard C. De Brier M. Bransby Best practice geotechnical characterization and pipe-soil interaction analysis for HPHT pipeline design 2015 Houston, Texas.
- [36] D. White, Z. Westgate, Y. Tian, Pipeline lateral buckling: Realistic modelling of geotechnical variability and uncertainty. Presented at the Offshore Technology Conference, 2014.
- [37] L. Zhao, S. Tjahyono, E. Tan, C.H. Do, Back analysis of measured as-laid pipeline embedment in soft clay. Presented at The The Twenty-fifth International Ocean and Polar Engineering Conference, 2015.